AN ABSTRACT OF THE THESIS OF

Nicolas Roussel for the degree of Master of Science in Electrical & Computer Engineering presented on March 27, 2003. Title: Advanced Image Segmentation, and Data Clustering Concepts applied to Digital Image Sequences featuring the Response of Biological Materials to Toxic Agents.

Abstract approved: Redacted for Privacy

Wojtek J. Kolodziej

Image segmentation is the process by which an image is divided into number of regions. The regions are to be homogeneous with respect to some property. Definition of homogeneity depends mainly on the expected patterns of the objects of interest. The algorithms designed to perform these tasks can be divided into two main families: *Splitting Algorithms* and *Merging Algorithms*. The latter comprises seeded region growing algorithms which provide the basis for our work.

Seeded region growing methods such as Marker initiated Watershed segmentation depend principally on the quality and relevance of the initial seeds. In situations where the image contains a variety of aggregated objects of different shapes, finding reliable initial seeds can be a very complex task.

This thesis describes a versatile approach for finding initial seeds on images featuring objects distinguishable by their structural and intensity profiles. This approach involves the use of hierarchical trees containing various information on the objects in the image. These trees can be searched for specific pattern to generate the initial seeds required to perform a reliable region growing process. Segmentation results are shown in this thesis.

The above image segmentation scheme has been applied to detect isolated living cells in a sequence of frames and monitor their behavior through the time. The tissues utilized for these studies are isolated from the scales of *Betta Splendens* fish family.

Since the isolated cells or chromatophores are sensitive to various kinds of toxic agents, a creation of cell-based toxin detector was suggested. Such sensor operation depends on an efficient segmentation of cell images and extraction of pertinent visual features.

Our ultimate objective is to model and classify the observed cell behavior in order to detect and recognize biological or chemical agents affecting the cells. Some possible modelling and classification approaches are presented in this thesis.

Advanced Image Segmentation, and Data Clustering Concepts applied to Digital Image Sequences featuring the Response of Biological Materials to Toxic Agents

by

Nicolas Roussel

A THESIS

submitted to

Oregon State University

in partial fulfillment of
the requirements for the
degree of

Master of Science

Presented March 27, 2003
Commencement June 2003

Master of Science thesis of Nicolas Roussel presented on March 27, 2003

APPROVED:

Redacted for Privacy

Major Professor, representing Electrical & Computer Engineering

Redacted for Privacy

Chair of Department of Electrical & Computer Engineering

Redacted for Privacy

Dean of Graduate School

I understand that my thesis will become part of the permanent collection of Oregon State University libraries. My signature below authorizes release of my thesis to any reader upon request.

Redacted for Privacy

Nicolas Roussel, Author

ACKNOWLEDGMENT

I would like to thank :

Prof. Wojtek Kolodziej (Department of Electrical and Computer Engineering),

Assoc. Prof. Frank Chaplen (Department of Bioengineering),

Assoc. Prof. Phil McFadden (Department of Biochemistry and Biophysics),

DARPA, NSF, the Cathalyst fundation,

Bertrand Boichon, Angela Teng (Graduate Student in Electrical and Computer Engineering),

The entire Cytosensor team,

for their help and support.

TABLE OF CONTENTS

TABLE OF CONTENTS (Continued)

TABLE OF CONTENTS (Continued)

LIST OF FIGURES

LIST OF FIGURES (Continued)

LIST OF FIGURES (Continued)

LIST OF APPENDIX FIGURES

ADVANCED IMAGE SEGMENTATION, AND DATA CLUSTERING CONCEPTS APPLIED TO DIGITAL IMAGE SEQUENCES FEATURING THE RESPONSE OF BIOLOGICAL MATERIALS TO TOXIC AGENTS

1. INTRODUCTION

1.1. Overview

Today most of the systems for detecting biological threats or dangerous chemical products are relatively specialized devices focused on a specific toxin or chemical molecule. A relatively new approach involves the observation of specific biological organisms (e.g. cells) which interact naturally to some biological or chemical threats (e.g. toxins). These biological organisms may respond in a observable sense and consequently provide data to the processing device, which can present this information in a meaningful manner. If the organisms to be observed react visually to the agent, image segmentation for the purposes of feature extraction is a required step.

This research project addresses general issues associated with the quantification and modeling of biological processes. The approached fields are principally cell segmentation, modelling and classification. The basis for our studies is a time sequence of images depicting the response of chromatophores to toxic and non-toxic agents.

The tissues utilized for these studies are isolated from the scales of *Betta Splendens* fish family (See Figure 1.1). Isolated cells or chromatophores sensitivity to various kinds of toxic agents suggested the possibility of creating a cell-based toxin detector. Most of our experiments were performed on image sequences featuring the time-dependent cell

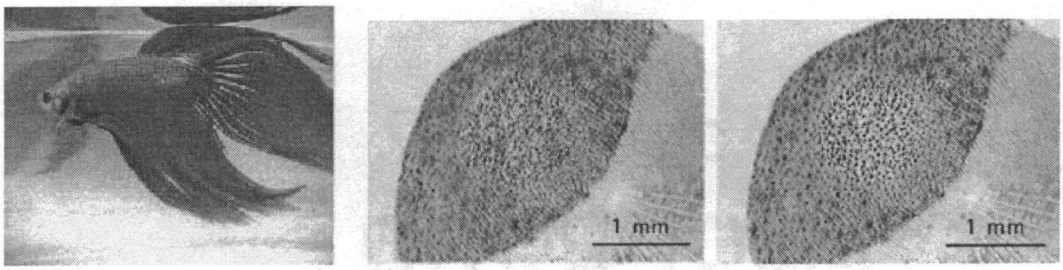

(a) (b)

FIGURE 1.1: (a):*Betta Splendens* fish (b):Fish scales

response. Nevertheless the methods that have been developed here are relatively generic and could easily be applied to other kinds of organic materials.

Chromatophores exposed to certain toxin classes react by altering their internal state (aggregation or dispersion of color bearing particles or chromatosomes). We will first briefly describe the cells from a biological point of view. A basic understanding of the physical processes involved in the cell reaction may provide us with some insights about the cell dynamics and help us in our subsequent tasks of quantification, modeling and prediction.

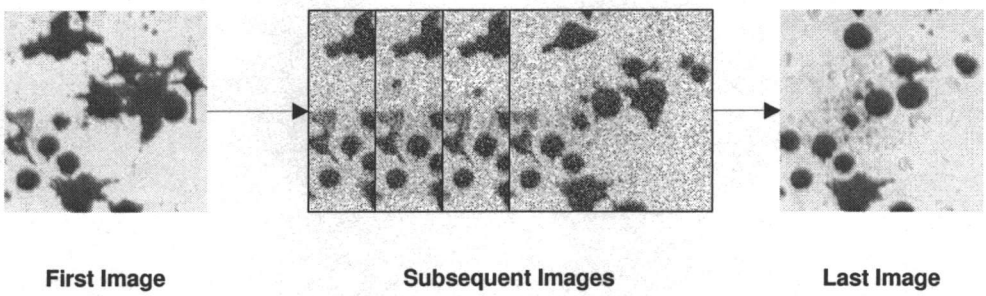

FIGURE 1.2: Sequence of images featuring the response of living cells

Measurement of the cell evolution is based on a sequence of RGB images taken at a constant sampling rate (See Figure 1.2). Our first task is to reduce the RGB image sequence into a comprehensive set of features. This require the use of advanced Region-based segmentation strategies for cell detection and tracking. Knowing the location of each individual cell in time allows to compute a set of time based features.

Finally, these extracted time series of features can be used for high level modeling, detection and identification.

1.2. Cell response: Biological understanding

A eukaryotic cell is composed of a nucleus surrounded by cytoplasm, which contains various kinds of organelles enclosed inside the cell membrane. Mechanical support is provided by the cytoskeleton which is a complex network of protein filaments that extend throughout the cytoplasm (See Figure 1.3).

It has been established experimentally that chromatophore organelles called chromatosomes are equipped with bound motor proteins which can move them along the cytoskeleton (Microtubule or actin filaments).

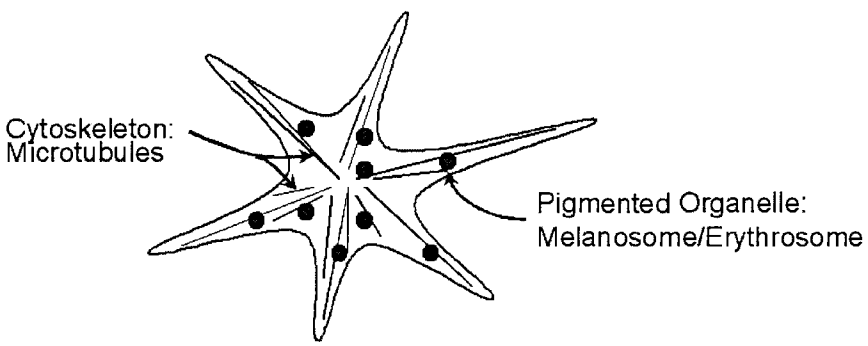

FIGURE 1.3: Inside schematic view of Chromatophore cells

From an image processing point of view, what we see are round shaped objects, the color of which ranges from black to red. What we actually see are aggregates of organelles called chromatosomes. At a given pixel location, color and intensity indicates the local chromatosome density.

Under normal conditions, chromatosomes are uniformly spread within the bounds of the cell membrane. The different pigmentation of the cells allows us to divide Chromatophores into 2 sub-cathegories: Melanophores (black) and Erythrophores (red). When the cell membrane comes in contact with certain toxic agents, membrane bound receptors are activated, they carry the information into the cytoplasm and trigger chemical signaling pathways. Typically, two kinds of behavior are observed.

- No reaction

  The cell is not sensitive to the external agent or the effect is not visible.

- Aggregation/Dispersion

  The bound motor proteins of chromatosomes are activated resulting in their migration along the cytoskeleton toward the center or the periphery of the cell (See Figure 1.4).

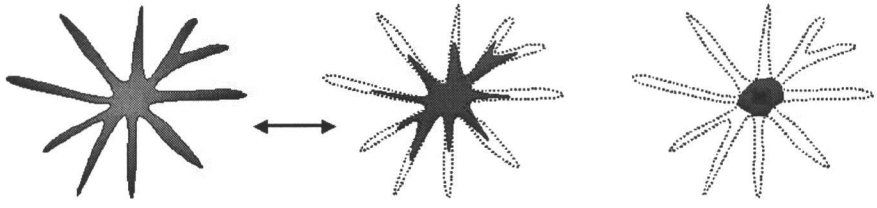

FIGURE 1.4: Response of Chromatophore cells

For our purpose, two facts are noted: 1) aggregation or dispersion processes do not involve visible modification of the 2-Dimensional cell membrane geometry - thus the visual change is atributed to progressive evolution of the Chromatosomes density

distribution; and 2) Many agents interact at receptor sites on the cell surface nad the information is carried toward the cell center using internal signaling mechanism. Others penetrate the cell membrane and interfere with membrane associated processes or processes occurring within the cell proper.

1.3. Related work

This section reviews the current research related to the main topics addressed in this paper: Modeling of cell processes and Cell image segmentation.

1.3.1. Modeling of biological cell processes

The modeling of the various biochemical signaling pathways that allow the cell to receive, process and respond to information is a very active field of research, which is motivated by the need to understand the cell response to various chemicals. Such an understanding is of great interest for example to the pharmaceutical industry, nonlinear approaches such as Biochemical signalling networks [1] are designed to fully model the internal cell mechanisms. The ultimate purpose of these techniques is to design simulation tools that would make pharmaceutical research significantly more efficient.

More closely related to the topic of this paper is research that focuses on modeling specific observable cell behavior, namely the transport of Intracellular Particles. These phenomena have been studied from a macroscopic point of view and one-dimentional models were designed for a wide variety of organelles [2]. Most of this research focuses on precisely describing this phenomenon, which results in complex sets of equations with biologically oriented parameters.

Quantitatively assessing external factors based on organelles transport is under intensive research, but publications on this topic are still relatively sparse.

1.3.2. Cell image segmentation

Segmentation of images depicting the cells is crucial to understanding of the cell behavior. thus the field of region based image segmentation is of interest to us. A variety of generic techniques has been proposed and tested by segmenting images into regions of some common property. These techniques can be classified into two main classes:

- Splitting algorithms
- Merging algorithms

Some of these techniques are usually associated with specialized data structures. A large variety of techniques utilizes quadtree as an image descriptor, they are for the most part designed to detect and segment objects characterized by their uniform intensity or texture. Such an approach which is of great interest for image compression would not apply to the segmentation of complex dendritic objects with non-uniform density profiles.

In situations where the object structure is complex and where over-segmentation is not acceptable, it has been shown that some a priori knowledge of the objects to be extracted is required. In the case of overlapping and touching objects this requirement is even more critical. This leads to the specific field of *model based image segmentation* where many segmentation approaches applied to various object structures have been tried.

Some versatile approaches using deformable object models have been developed [3]. However they are, in practice, limited to relatively simple models. In the case of Chromatophore cells, the density profile of the organelle distribution can exhibit a great variety of configurations and has an inherent morphological complexity.

2. REGION BASED SEGMENTATION ON COLOR IMAGES

2.1. Introduction

The function of Region-Based Segmentation is to extract homogeneous, with respect to some properties, regions of an image. Definition of homogeneity depends mainly on the expected pattern of the objects that we want to extract. This task is important to image compression, pattern recognition, computer vision etc.

Numerous algorithms have been designed to perform segmentation tasks. Basically, these algorithms can be divided into two main families: *Splitting Algorithms* and *Merging Algorithm.* The later comprises seeded region growing algorithm which is a well known region-based segmentation method that segments intensity images into regions based on a marker set. As the name implies it is a procedure that groups pixels into larger regions. Border pixels are added to regions in an order that depends on the similarity between the pixels and the marked region. Performance of this method is therefore highly dependent on the initial seeds choice.

The automatic generation of a marker set is a broad area of research which involves object detection. This approach always requires specific knowledge or models of the objects that we want to detect. In the case of images containing several objects of different shapes and intensity that together form compound objects, detection can be a very complex task that is often assisted manually by a user.

In this paper, we present a generic approach for automatic object detection. This method is best suited to gray scale images where objects are to be distinguished by their low intensity profile (high light absorbtion or low light transmission factor). This method involves the generation of a hierarchical tree containing information concerning the structure and intensity of an image. Object detection can be performed by searching this tree for specific patterns.

2.2. Problem formulation

Let I be an image that we wish to segment, $I(x, y)$ is the value of the pixel at the coordinates (x, y). I can be ideally divided into an optimal set S of N regions: $A_i, i = 1...N$: $S = \{A_i, i \in \{1...N\}\}$. A_1 will be the background region and $A_i, i = 2...N$ will represent the regions of the $(N - 1)$ objects contained in the image.

Our objective is to generate a marker set $S' = \{A'_i, i \in \{0...N\}\}$ such that for each optimal region $A_i, i \in \{1...N\}$, $A'_i \subset A_i$. A'_0 is the region of unknown class modeling the ambiguity of the object detection process. This ambiguity will be resolved by the seeded region growing segmentation algorithm.

The method discussed in this paper requires specific knowledge about the objects to be detected, and the performance of the algorithm depends on this knowledge relevance. Knowledge of the expected objects can be extensive or reduced to simple facts such that {*"Each Object corresponds to a local intensity minima"* }.

Figure 2.1 shows a sample image where this method can be applied. It features a population of cells called *Chromatophores* which can be found in the scales of *B. Splendens* fish.

This image highlights many object detection issues such as:

- The image contains cells of various shapes and intensity profiles.
- Some of the cells form aggregate, *compound objects.*

Here the Chromatophore cells are the objects that we wish to detect. They can be divided into multiple families. For our purposes we focus on Erythrophores and Melanophores. Among these two families, cells can come in several configurations. Figure 2.2 and 2.3 show the various cell types and configurations that the object detection algorithm may encounter. In Chapter 3 we will present the result of segmentation obtained for these chromatophore images.

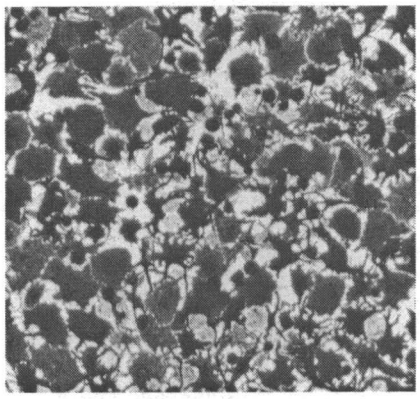

FIGURE 2.1: Chromatophore and melanophore cells

Erythrophore Cells	
Dendritic Configuration 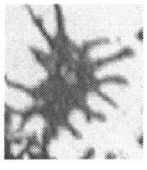	Reddish dendritic medium sized objects
Compact Configuration 	Reddish solid and big objects
Aggregated Configuration 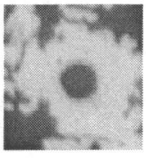	Dark, small and round shaped objects

FIGURE 2.2: Presentation of the various configurations of Erythrophore and Melanophore cell families

Melanophore Cells	
Dendritic Configuration 	Black dendritic medium sized objects
Compact Configuration 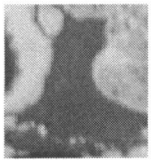	Black solid and big objects
Aggregated Configuration 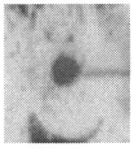	Dark, small and round shaped objects

FIGURE 2.3: Presentation of the various configurations of Erythrophore and Melanophore cell families

2.3. Hierarchical approach to region based segmentation

The proposed approach to perform a reliable region based segmentation when the cell structure is not precisely defined can be decomposed into 3 successive steps.

- Building the hierarchical tree that we might call *hierarchical structure descriptor.*
- Searching the tree for specific pattern to generate the objects markers.
- Performing the seeded region growing to segment the initial image.

2.3.1. *Building the hierarchical structure descriptor*

The hierarchical structure descriptor is very closely related to a region based image representation called *Max-Tree* [4]. This structure has been first introduced as an efficient way to implement *Connected Operators* [4] that are filtering algorithms inspired by mathematical morphology that eliminate part of the content of an image leaving the boundaries information unchanged. In this paper, we describe a variation of *Max-Tree* that we will use for object detection purposes.

The first step toward building the hierarchical structure descriptor is Image quantization. The input image I is to be reduced to an image L of N color labels, each one of them corresponding to a representative color class. Efficient algorithms that divide a population of pixels into a number of classes with respect to some minimal class variance constraints are available [5].

We assume that labels corresponding to representatives colors are sorted with respect to their decreasing intensity.

Image L can be viewed as N binary images $\{B_i, i \in \{1...N\}\}$, such that $B_i(x,y) = 1$ if $L(x,y) = i$. L is used to generate the cumulative binary image collection: $\{Bc_i, i \in \{1...N\}\}$ which is created as follows (see figure 2.4):

$$Bc_1 = B_1 \ominus Str \oplus Str$$

$$Bc_i = (Bc_{i-1} + B_i) \ominus Str \oplus Str$$

Notice that we incorporated morphological opening using a structuring element Str. This process is very similar to a dynamic multi-thresholding that would be applied to a gray scale image.

Alternatively cumulative binary images collections can be represented as a cumulative label image LB of N labels defined as:

$$LB(x) = 1 \text{ if } Bc_1(x) = 1$$

$$LB(x) = i \text{ if } Bc_i(x) = 1 \text{ and } Bc_{i-1}(x) = 0 \ ,i = 2 \dots N$$

The second step of this process involves connected components labelling applied to the cumulative binary image collection (Figure 2.5). This produces N sets of regions: $\{RegionSet_i, i \in \{1...N\}\}$ where $RegionSet_i$ contains the n_i connected compo-

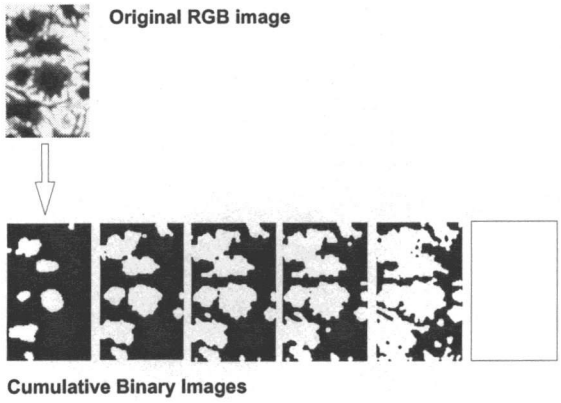

FIGURE 2.4: Original RGB image and cumulative binary image collection ($N = 6$)

nents $\{Cc_j^i, j \in \{1...n_i\}\}$ from the cumulative binary image Bc_i. Notice that $RegionSet_N$ contains only one connected component comprising the whole image thus $n_N = 1$.

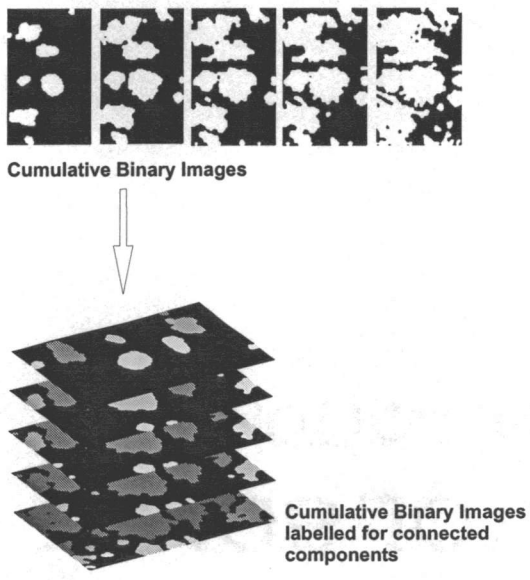

FIGURE 2.5: Labelling of the cumulative binary image collection

The hierarchical structure descriptor is a tree containing $(\sum_{i=1}^{N} n_i)$ nodes (See Figure 2.6). The root node correspond to the Connected component Cc_0^N and represents the entire image. Given a node corresponding to region Cc_j^i its children are regions from the labelled image $\{Cc_k^{(i-1)} | Cc_k^{(i-1)} \subset Cc_j^i\}$.

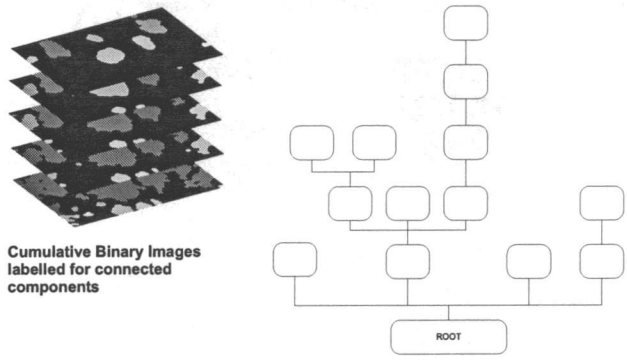

FIGURE 2.6: Hierarchical Tree building process

2.3.2. Pattern searching in the hierarchical structure descriptor

The hierarchical structure Tree is a high level descriptor of the image objects. It contains information on both the shapes and color/intensity of the objects in the image.

It can be used to perform various tasks such as object detection or recognition. The simplest use of the tree would be the search for local maxima and use them as seeds for region growing segmentation (in our case marker initiated Watershed segmentation). A local maxima would correspond to the top of the branch of a tree. For basic denoising purpose we can introduce minimal area criterion for those seeds. Some practical segmentation results using this simple method are presented in Section 2.6. Figure ??.

Based on some a priori knowledge of the of objects the tree can be processed using split and merge approaches and next be searched for specific pattern. The search result can be used to generate a more relevant marker set for region growing segmentation.

Knowledge of the object structures that we wish to segment can be summarized by ranges of tolerance of various region node properties:

- We can define general and specific Color and intensity tolerance ranges. In our experimental tests we did not use extensively this option. Instead we here focused on performing a light independent structure based object detection.
- The Area of region node must be within a tolerance interval. We can define a general Area range for all the cell types and configuration [$GeneralMinimalArea$, $GeneralMaximalArea$]. Some area ranges specific to the cell type and configuration can also be devised.
- Additional structure oriented features can be used to assess the cell type and configuration such as Object $Solidity$, $ConvexArea$, etc.

2.4. Segmenting Chromatophore cells

In this section, we apply the generic concept of Hierarchical region based segmentation discussed in section 2.3. to images depicting chromatophore cells. Our task is to design proper tree processing and pattern searching algorithms relevant to detecting chromatophores.

2.4.1. Chromatophore density map

The grayscale images showing chromatophores are obtained by the image acquisition system. These images provide us with a rough estimate of the organelle (chromatosome) density distribution within the field of view. There are two major drawbacks of using this estimate.

- The gray scale level of the image can vary depending on the light intensity.
- At a given pixel location gray scale level and local chromatosome density are related through a non linear mapping function. This can make statistical analysis of chromatosome population difficult.

In this section we define a consistent estimator of the chromatozome density map using the LIP (*Logarithmic Image Processing*) model shortly presented in section D.

2.4.1.1. The image acquisition system

An example of image acquisition system is shown in Figure 2.7. A source emits light that is transmitted across two stacked mediums: the fluidic medium **Mf** and the chromatophore medium **Mc**. The transmitted light is captured by the camera and converted to a gray scale image f.

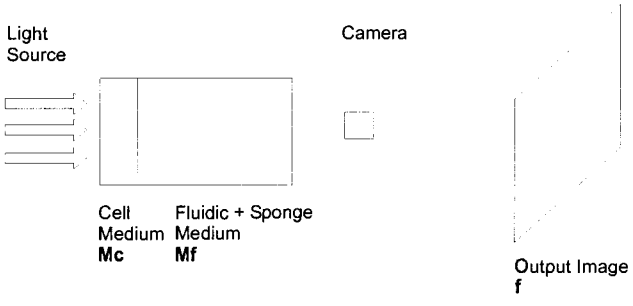

FIGURE 2.7: Schematic view of the acquisition system

The chromatophore medium **Mc** is a simplified view of the chromatosomes population in the field of view. It is characterized by its transmission factor T_c: $T_c(x) < 1$ if some chromatosomes are located at x, $T_c(x) = 1$ if no chromatosome is located at x. The fluidic medium **Mf** represents all the materials other than the chromatosomes. Our objective is to minimize the influence of the fluidic medium.

According to LIP formalism, the output image f can be seen as the result of the LIP addition of two images f_c and f_f:$f = f_c(+_{LIP})f_f$ where f_c is the image obtained when only the chromatozomes medium is present and f_f is the image obtained when only the fluidic medium is present.

2.4.1.2. Filtering out the influence of the fluidic medium

The information made available to us by the acquisition system is an image $f = f_c(+_{LIP})f_f$ obtained by the transmission across the chromatophore and fluidic medium. In practice only f_c is of interest .

Theoretically, obtaining f_c could be as simple as performing the LIP substraction $f(-_{LIP})f_f$. Unfortunately f_f is not directly available and needs to be estimated.

Let the background B of an image be a set of pixels where no chromatophore is located. According to our previous assumption, we know that $T_c(x) = 1$, $f_c(x) = 0$ if $x \in B$. Therefore, if $x \in B$, $f(x) = f_f(x)$. The estimate $\hat{f}_f$ of f_f can be obtained by extrapolating the values of f_f at the location $\bar{B}$.

Since $\hat{f}_f$ is available, it is relatively straightforward to obtain an estimate of f_c:$\hat{f}_c = f(-_{LIP})\hat{f}_f$

2.4.1.3. Software based light stabilization

Basically, increasing the light input is equivalent to decreasing the thickness of the medium using LIP multiplication $\times_{LIP}$. Stabilizing light input involves the task of adjusting the background intensity to a target gray scale level N using the $\times_{LIP}$ operator. The LIP multiplier n can be obtained simply using the following formula.

$$n = \bar{\hat{f}}_f \times_{LIP} \frac{1}{N} \tag{2.1}$$

This leads to a stabilized image f_{stable}:

$$f_{stable} = f \times_{LIP} n \tag{2.2}$$

Notice that to obtain the LIP multiplier factor, we only used $\hat{f}_f$ instead of f. The reason for this is that the background (obtained by transmission over the fluidic medium) has an average transmission factor that is relatively constant because the volume of liquid is standardized in our experiments.

2.4.1.4. Estimating the chromatosomes density

Estimating the image f_c is an important step toward the creation of a density map. However, it can be demonstrated that $\hat{f}_c$ is not linearly related to the actual density of chromatophore d.

Let us first discuss the physical meaning of $\hat{f}_c$ and $\hat{T}_c$. We consider a pixel at location x in the medium.

- If a unitary volume v of chromatozomes is located at x 2.8 (a) then
  $f_c^u(x) = U$
  $T_c(x) = 1 - \frac{U}{M}$
- If a volume kv of chromatozomes is located at x (Figure 2.8 (b)) then
  $f_c(x) = M(1 - (1 - \frac{U}{M})^k)$
  $T_c(x) = (1 - \frac{U}{M})^k$

The estimate of the chromatophore density d can be theoretically obtained by the following formula:

$$d = \frac{log(1 - \frac{f_c}{M})}{log(1 - \frac{f_c^u}{M})} \tag{2.3}$$

This formula requires that the grayscale level f_c^u obtained by transmission across a unitary volume of chromatophores is known. However, under stable light conditions, this value is assumed to be constant and a reliable estimate of d can be obtained as.

$$\hat{d} = -log(1 - \frac{f_c}{M}) \tag{2.4}$$

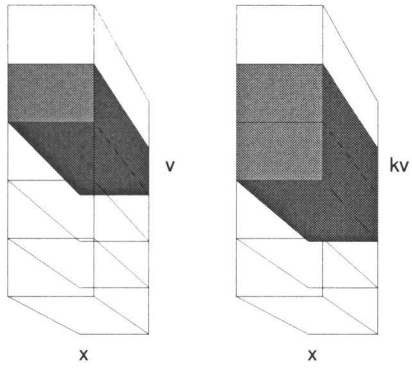

FIGURE 2.8: Medium volume schematic view at location x

2.4.2. Description of cell population

Hierarchical region based segmentation provides us with a convenient way to obtain reliable local intensity minima from a color image. However the major advantage of this method is that this high level image descriptor can also be used to search for specific object patterns based on some a priori knowledge of the objects. Our task is to precisely define the chromatophore cells in the context of the acquired images.

From the known biological properties of the cells (Section 1.2.), we know that the objects that we wish to segment are aggregates of Chromatosomes. At a given pixel location, color and intensity indicates the local Chromatosome density. Examples of cells images and density profiles can be seen in Figure 2.9.

Mathematically, a chromatophore cell can be defined by its membrane geometry and the chromatozome density distribution within the membrane. Due to the ellipsoid like shape of the membrane, this distribution can be roughly approximated by a gaussian density distribution. As a result the chromatozome density map can be seen as a mixture model composed of a number of gaussian density distributions.

Pigmentation of organelles is also an important feature since it permits the differentiation between Erythrophores (red) and Melanophores (black).

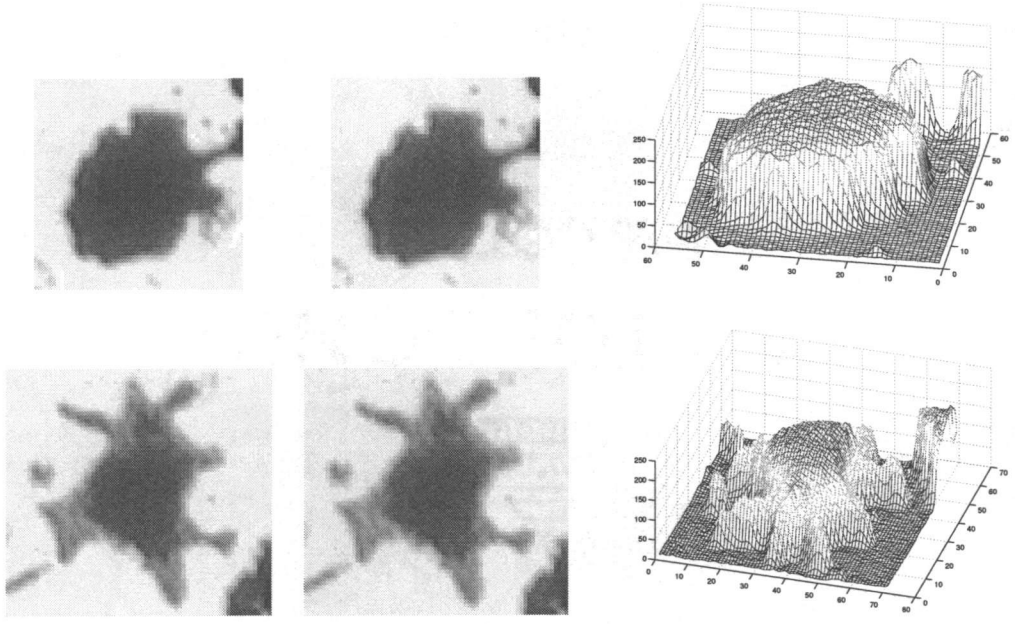

Color Image gray scale image density profile

FIGURE 2.9: Cell images and their density profiles

The major advantage of hierarchical Region based segmentation is that it can be used to search for specific object patterns based on some a priori knowledge of the objects. We divide object knowledge into two categories: **Hard parameters** and **Soft parameters**.

2.4.2.1. Hard parameters

We call **Hard parameters**, any information provided by the end user. Such a set of information is supposed to be short, comprehensive, and valid for the broadest range of experimental conditions. In our implementation, we reduced this set to simplest structural cell properties:

MINIMAL CELL AREA

MAXIMAL CELL AREA

2.4.2.2. Soft parameters

Soft parameters on the other hand are not provided by the end user and only apply to the image currently under consideration. The general idea is to perform a sub-optimal region based segmentation on the current image, select the region that meets the Hard parameters requirement and derive from those regions an extensive set of object properties that will be used in the next tree processing iteration.

Consider the set S of M regions $S = \{R_i, i = 1 \dots M\}$. Using the Hard Objects parameters we can define exclusion rules to filter out the region set S thus creating a set S' of N valid object regions $S' = \{R'_j, j = 1 \dots N\}$ (See Figure 2.11 and 2.12).

As soft parameters, we could use order 0 and 1 moments of various quantities such as color, Intensity, Chromatozome weight etc. But in our approach we focus on computing some density distributions of the region pixel values in the cumulative label image LB (See section 2.3.1.).

Each region R'_j from S' is a set of pixel locations, which can be characterized by their associated value in the map LB and their radius relative to the geometric centroid of the corresponding region. From this we can devise the density distributions:

- $P(clabel = l | radius = r)$
- $P(radius = r)$
- $P(radius = r | clabel = l)$ (Figure 2.13)
- $P(clabel = l)$(Figure 2.14)

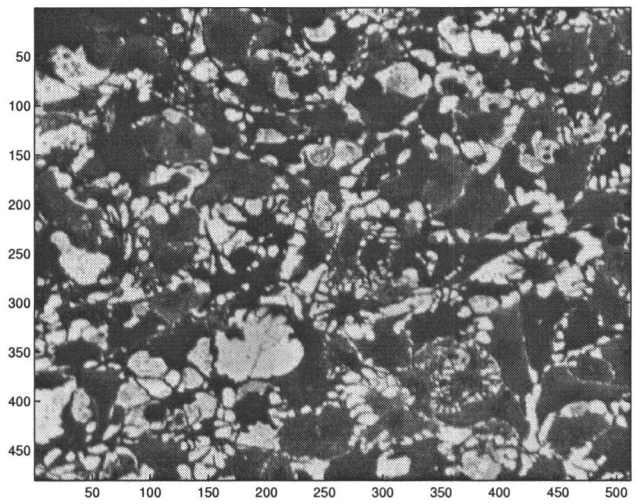

FIGURE 2.10: Original RGB image

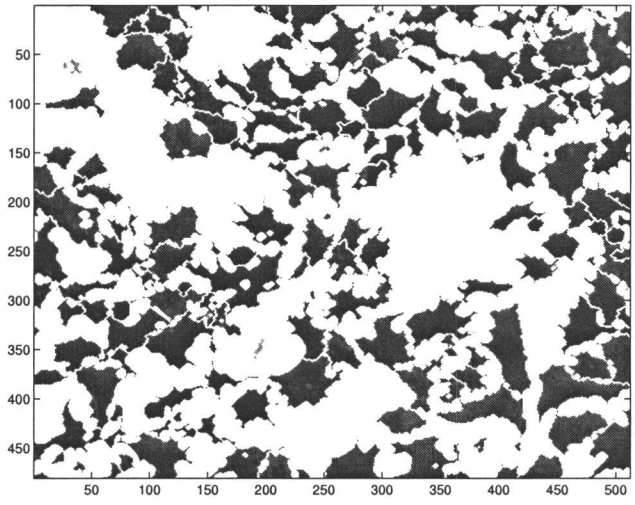

FIGURE 2.11: selected Objects in color space

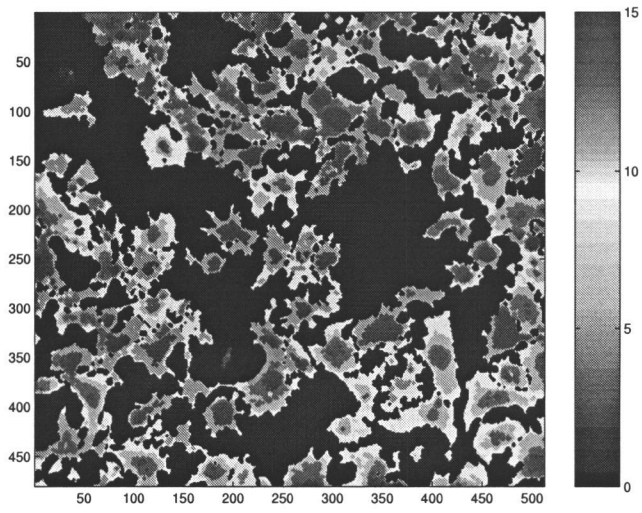

FIGURE 2.12: selected Objects in cumulative label space

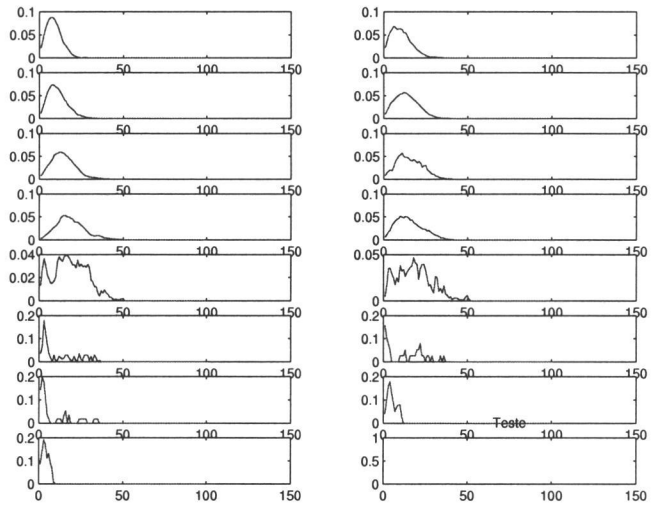

FIGURE 2.13: $P(radius = r|clabel = l)$

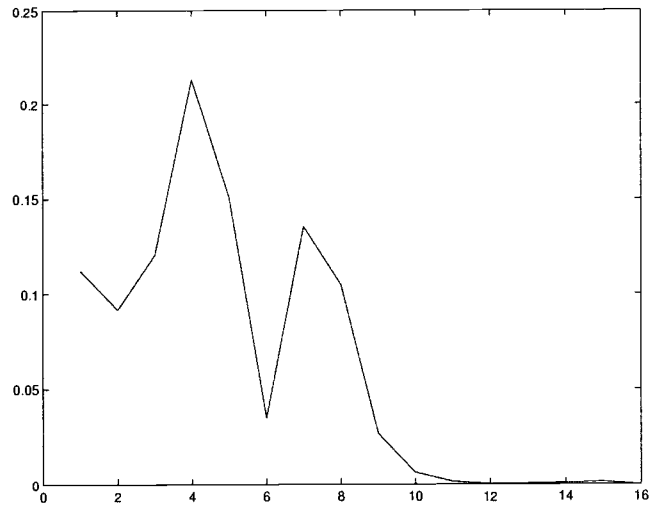

FIGURE 2.14: $P(clabel = l)$

2.4.3. Split and merge approach applied to the hierarchical Tree

Each node of the hierarchical tree represents regions of the image. In theory, a node region may coincide with one or several cells. For the latter, it is expected that children nodes from lower levels will allow the identfication of each individual cell (Figure 2.15).

However the following may arrise:

- A node which coincides with a single cell can have several childrens thus wrongly implying that this node is composed of several cells (Figure 2.17).
- Children of a node which coincide with several cells may not allow the identfication of each individual cells (Figure 2.16).

To resolve those problems, we need to devise split and merge strategies applied to the nodes of the tree. Given a node region R corresponding to k actual cells, we intend to divide R into k sub regions $\{c_i, i = 1 \ldots k\}$, each one of them corresponding to a single cell.

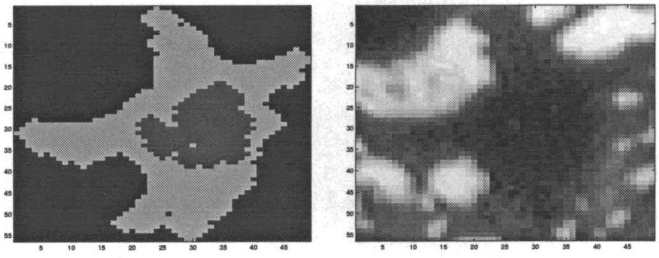

Root/Children view Gray scale Image

FIGURE 2.15: Best case scenario

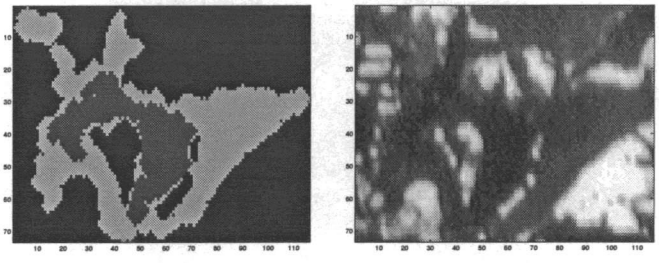

Root/Children view Gray scale Image

FIGURE 2.16: Root split required

R can be considered as a collection of points in 2D together with their weights taken from the chromatosome density map (see Section 2.4.1.). Assume that cells can be modeled by a gaussian density distribution, then R can be seen as a mixture model composed of k chromatosome distributions. Our objective here is to identify each one of these distribution.

A very well suited method for this task is the Gath-Geva (GG) clustering algorithm [6] since it assumes that each cluster is a realization of a normally distributed random variable. The main issue in this approach is that the number of clusters must be known a priori and given as a parameter. To perform an optimal clustering, we must apply the GG process with several values of k, retaining the partition that best fits the objects properties.

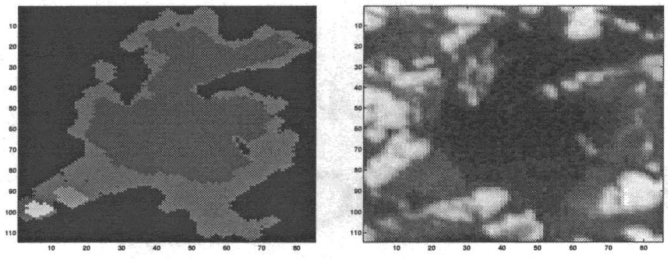

Root/Children view Gray scale Image

FIGURE 2.17: Splitting and merging required

Given a partition P_N of R into N sub regions $P_N = \{c_i, i = 1 \ldots N\}$ our main task is to define a clustering quality index Q. In our approach, the estimator is primarily based on the soft parameters extracted previously and discussed in Section 2.4.2.2..

As mentioned previously each sub region c_i from P_N is a set of pixel location, characterized by their associated value in the map LB and their radius relative to the geometric centroid of their corresponding region. Therefore the partition becomes a collection D of M pixels represented by their radius and cumulative label: $D = \{(r_i^N, l_i^N), i = 1 \ldots M\}$.

As a quality index we use:

$$Q(P_N) = \sum_{i=1}^{M} P(radius = r_i^N | clabel = l_i^N) P(clabel = l_i^N) \tag{2.5}$$

This estimator will ensure that the partition with the highest "probability" is selected. Figure 2.18 shows the experimental results of this approach.

The output of the GG algorithm is a partition map that is used to define splitting and merging rules. These rules can be applied recursively to the processed node and its children.

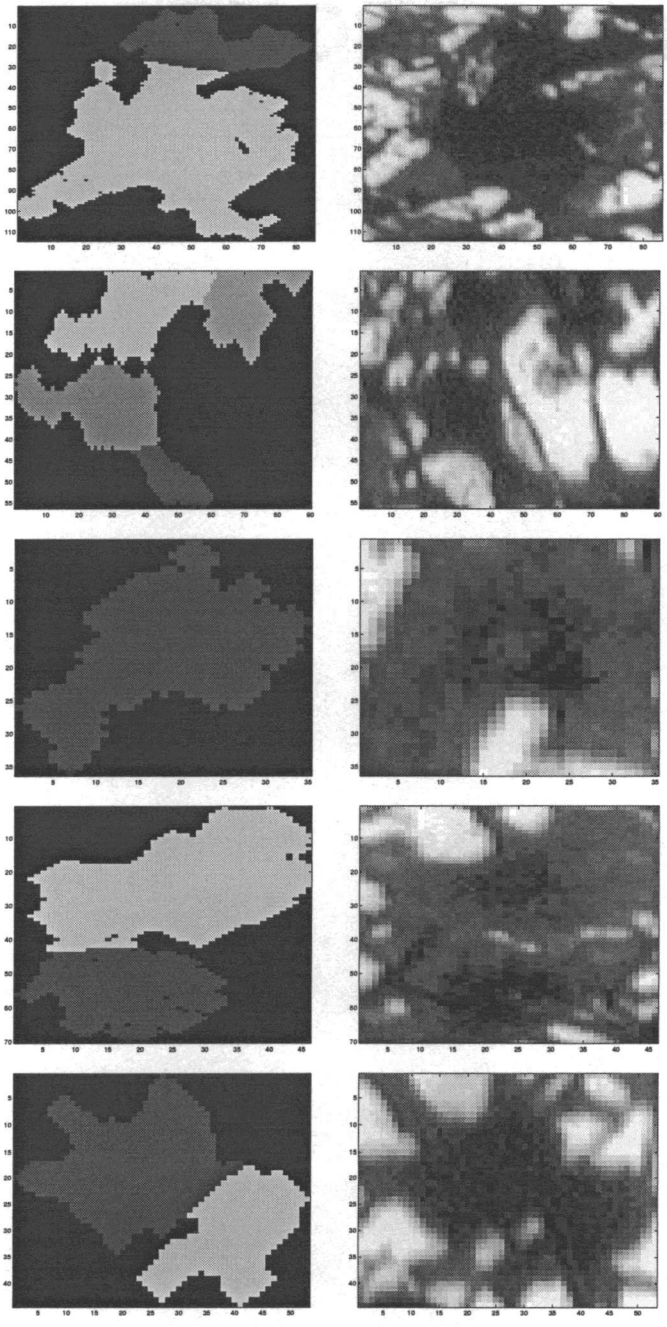

Selected partition Gray scale Image

FIGURE 2.18: Node partition Results

2.4.4. Searching for chromatophore patterns in the hierarchical Tree

In the Hierarchical Tree, we are going to check each individual node for specific patterns. From the tree we will consider a node from level i and its immediate successors form level $(i + 1)$. This procedure forms the subtrees that will be next checked for patterns. Examples of these subtrees can be seen in Figure 2.19.

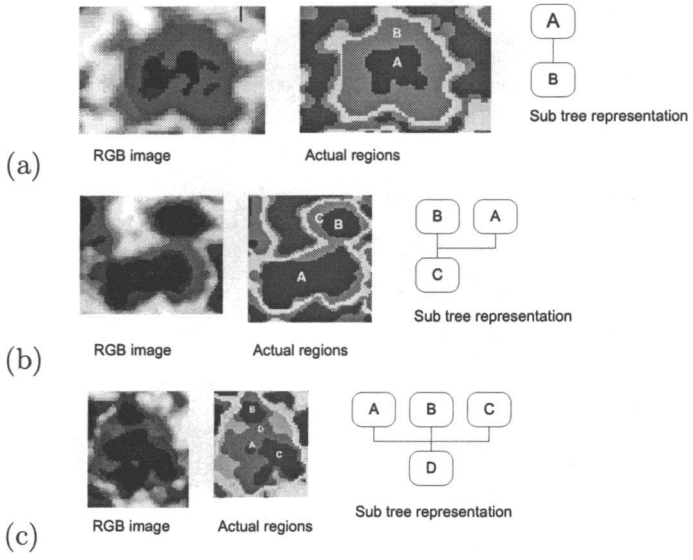

FIGURE 2.19: Examples of Objects associated with their sub-trees

In our implementation, most of the computational complexity is in the split and merge processing of the tree. As a result we will search our enhanced tree for simple local minima patterns (See Figure 2.19 (a)).

2.5. Segmentation processing loop

in Section 2.4.2.2., we described **Soft parameters** as region information extracted from a sub-optimal segmentation of the current image. These soft parameters are then

used by the split and merge algorithm and yield an enhanced tree. From this enhanced tree, more relevant seeds can be extracted to perform a marker initiated region growing process such as Watershed segmentation.

Assuming that the new regions better describe the actual cell population, they could be used to refine the initial soft parameters and reiterate the segmentation process.

From these considerations, it is relatively straightforward to define a multipass segmentation process where the segmentation result would improve after each loop iteration (Figure 2.20).

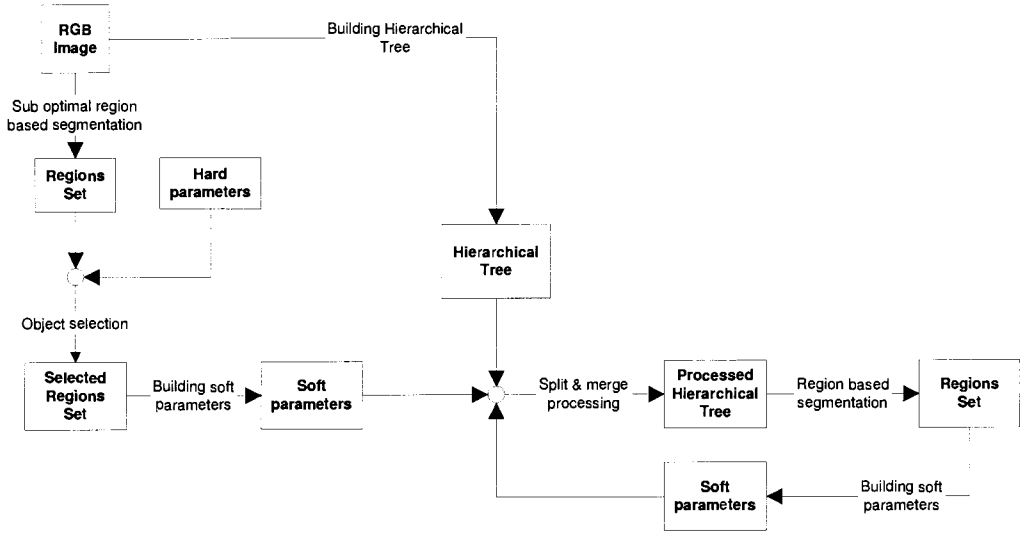

FIGURE 2.20: Diagram of the segmentation processing loop

This concept can be further extended in the case of image sequences where changes between two subsequent frames are limited.

2.6. Segmentation results

In this section, we present the result of our segmentation algorithm applied to a rather challenging image where distinction of individual cells is extremely difficult.

As hard parameters we selected:

MINIMAL CELL AREA=100

MAXIMAL CELL AREA=5000

To initialize the process, we performed a marker initiated watershed segmentation using local minima seeds from the tree.

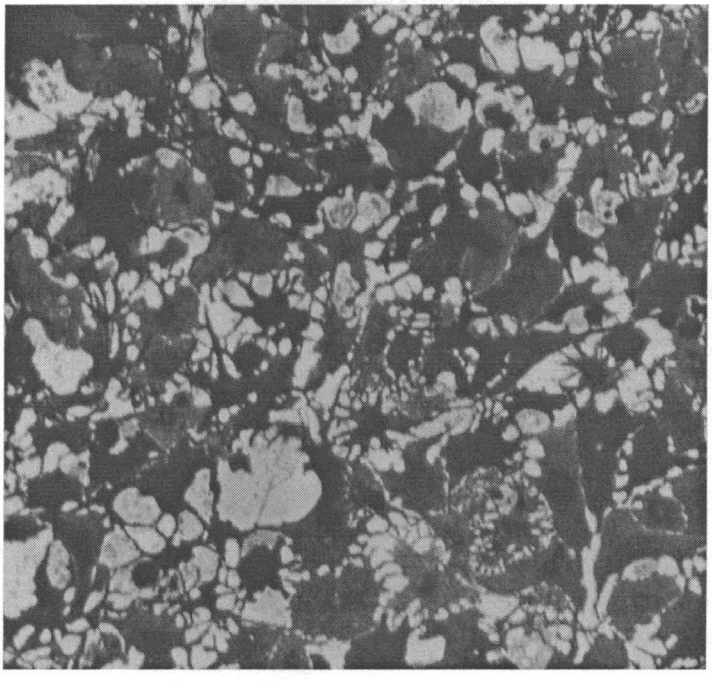

FIGURE 2.21: Original RGB image depicting a population of Chromatophores

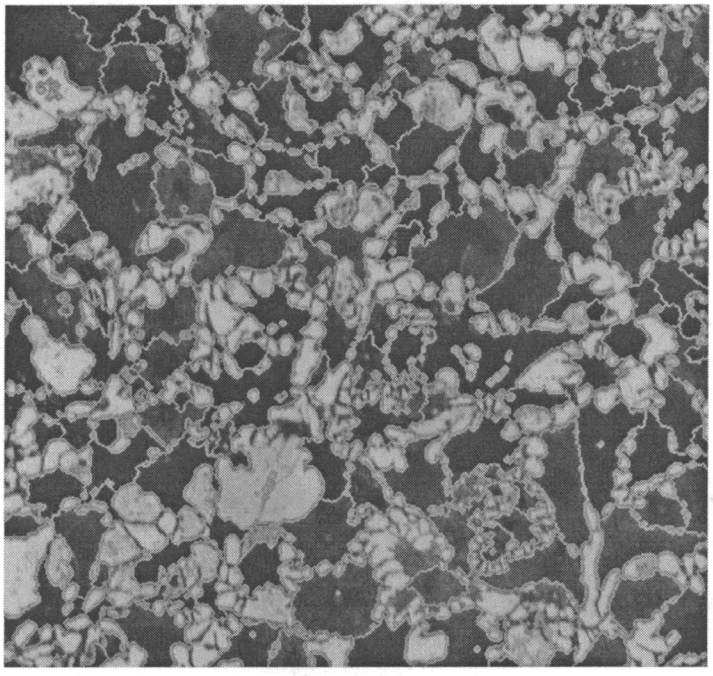

FIGURE 2.22: First pass segmentation result

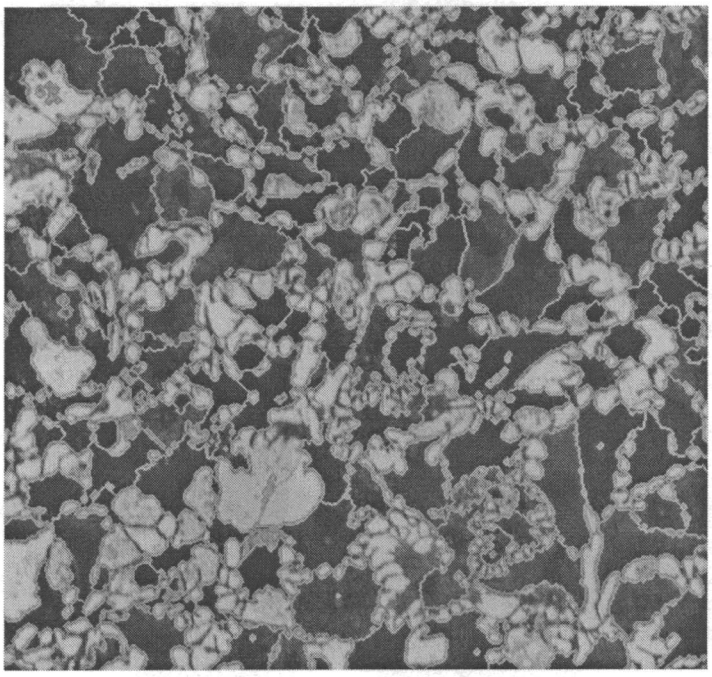

FIGURE 2.23: Second pass segmentation result

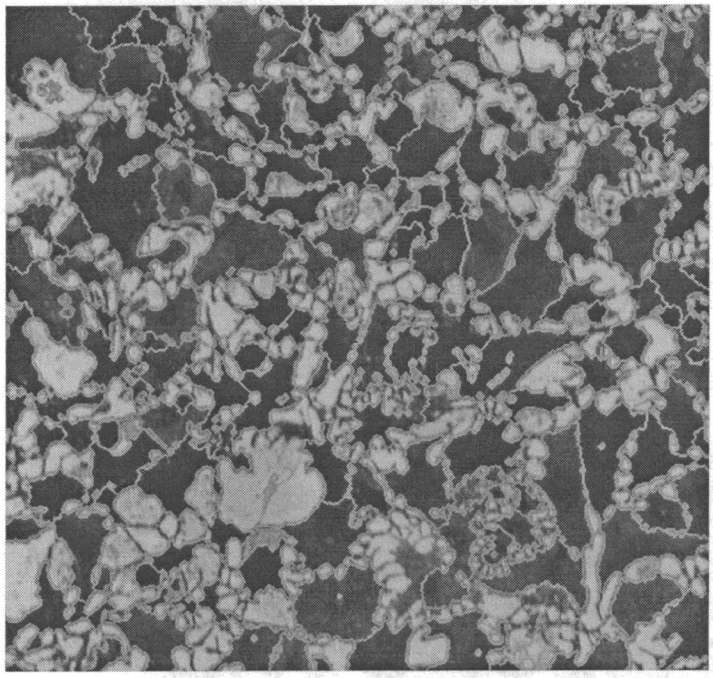

FIGURE 2.24: Third pass segmentation result

3. PROCESSING OF VIDEO SEQUENCES

The region based segmentation algorithm described in the preceding chapter applies to a single image. A simplistic approach would be to use this method for each image of the sequence. the cell tracking could be performed using for example the *Ungarian Algorithm* to assign to each object of an image a single successor from the next image according to some minimal cost criterion.

Such an approach although valid is very time consuming and does not fully exploit the inherent redundancy between images in a time sequence. Here we use a more efficient approach for dealing with both the image segmentation and cell tracking.

The general idea behind this method is that changes of cell size and location from one image to the next are relatively small. Furthermore, upper bounds of these changes can be devised based on the biological facts. Therefore region based segmentation of an image can be performed in a relatively straightforward manner by using the segmentation result from the preceding image as markers.

This method has proven to be reliable and relatively fast, however it needs to be further refined to be able to deal with some special situations:

- Translation of the image focus:

  This particular phenomena shows as a global translation of the field of view. In our implementation, we used a crude correlation based tracking strategy that should not be needed in stabilized operational conditions.

- Fast cell migration:

  The observed cells are maintained in a fluidic environment. Chromatophores are surface adherent, but it is not uncommon to see some cells moving freely in the fluidic medium.

3.1. Basic concepts

Let us first assume that we are observing a cell population under optimal condition, i.e. that we are not confronted with such disturbances as change of the image focus or fast cell migration. The only behavior that is expected from the chromatophores is organelle aggregation or dispersion.

First, these cell evolution processes are described and models are proposed. Next the actual sequential segmentation process is discussed.

3.1.1. Expected cell behavior

When the membrane of a cell comes in contact with some toxic agent, two kinds of behavior can be expected: Chromatosomes Aggregation or Dispersion.

In the case of Aggregation (See Figure 3.3 and 3.4), the organelles migrate along the cytoskeleton toward the center of the cell. Considering the microtubules configuration inside the membrane, this movement can be considered as radial following a straight line from the periphery toward the center of the cell.

This behavior can be seen as an apparent change in the cell are, or in the image processing term as a morphological erosion of the cell binary map. The choice of the suitable structuring element S is important. While a disc shaped S could be perfectly valid for convex cells, it is likely that such S wrongly erases the dendrils of non-convex cells (See Figure 3.1).

A better choice would be to use a radially oriented structuring element T (See Figure 3.2).

Let us considering a region R_{t_1} of the frame taken at time t_1. The chromatozomes of this region are assumed to converge toward the center at speed v. If we want to compute the estimate of R_{t_2} at time t_2, then the eroding structuring element $T_{(X,Y)}$ applied at the location (X, Y) of R_{t_1} is mathematically defined as follows:

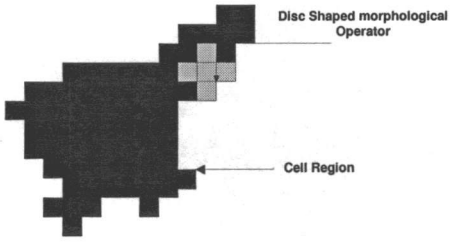

FIGURE 3.1: Use of a disk shaped structure element to simulate Aggregation

$$T_{(X,Y)}(x,y) = 1 \quad \text{if} \qquad -Yx + Xy = 0$$
$$\text{and } \sqrt{(X-x)^2 + (Y-y)^2} \leq v(t_2 - t_1)$$
$$T_{(X,Y)}(x,y) = 0 \quad \text{otherwise}$$

We assume in this formula that the center of the cell corresponds to the origin.

Notice that in this case we use a dynamic structure element to perform the erosion, which can be computationally expensive. In the case of large regions it is preferable to process the image in the polar coordinates with static T.

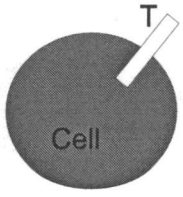

FIGURE 3.2: Cell erosion using a radially oriented structuring element T

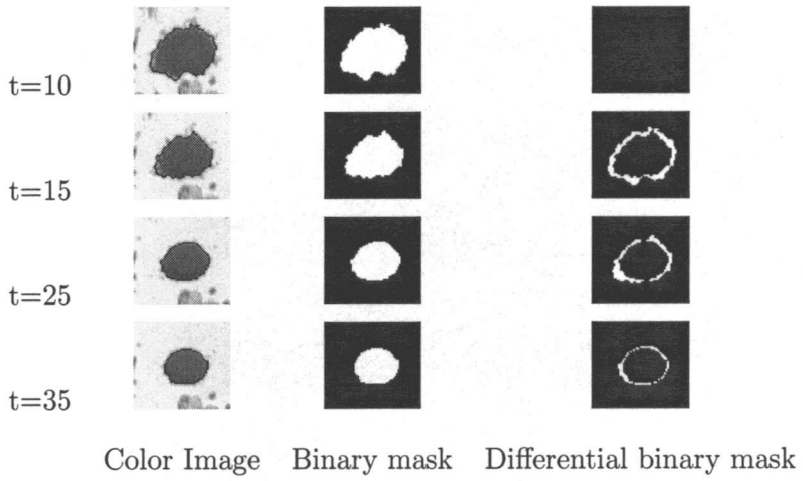

FIGURE 3.3: Aggregation of a compact chromatophore

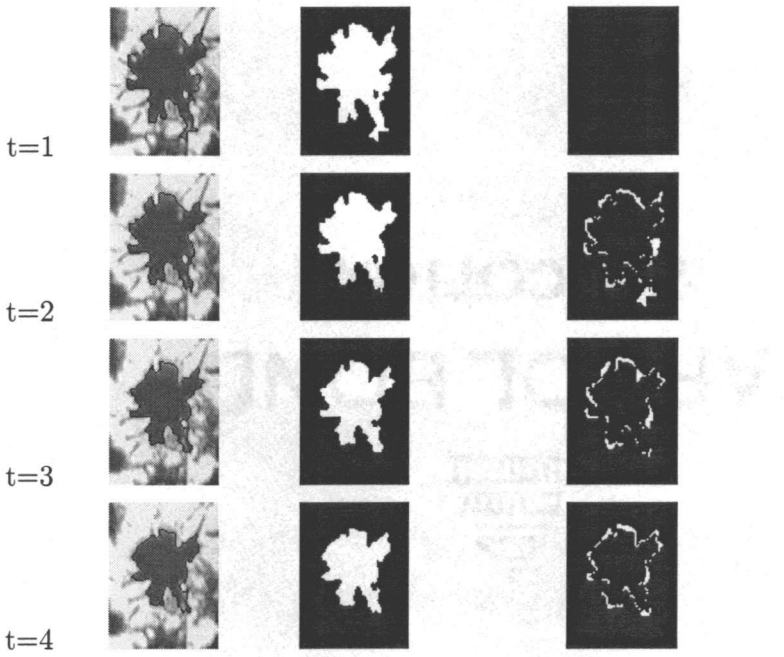

FIGURE 3.4: Aggregation of a dendritic chromatophore

In the case of Dispersion (See Figure 3.5 and 3.6), the organelles migrate along the cytoskeleton toward the periphery of the cell. This movement can be considered also as radial following the straight line from the cell center and towards its periphery.

We could simulate this behavior in a similar way as for the aggregation process using the same type of structuring element T, but performing morphological dilatation instead of erosion.

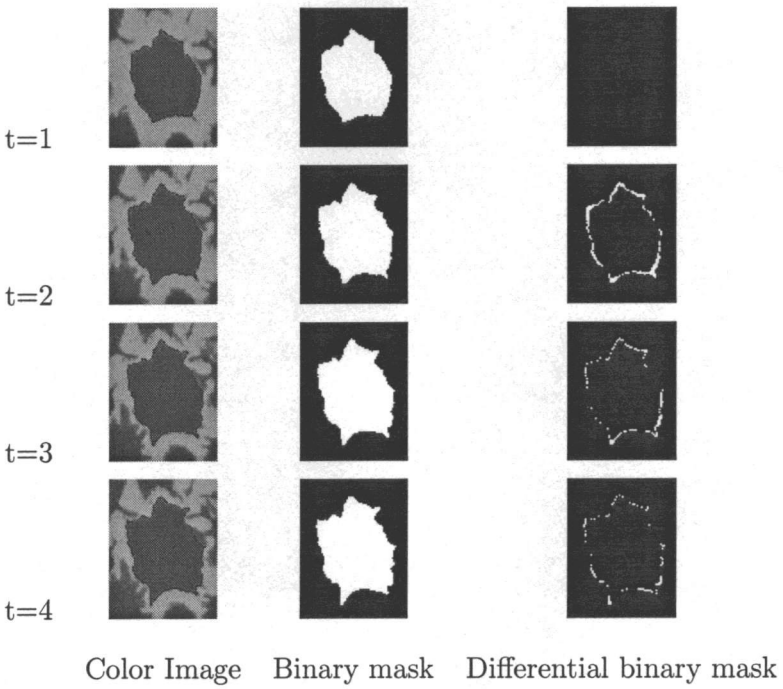

FIGURE 3.5: Dispersion of a compact chromatophore

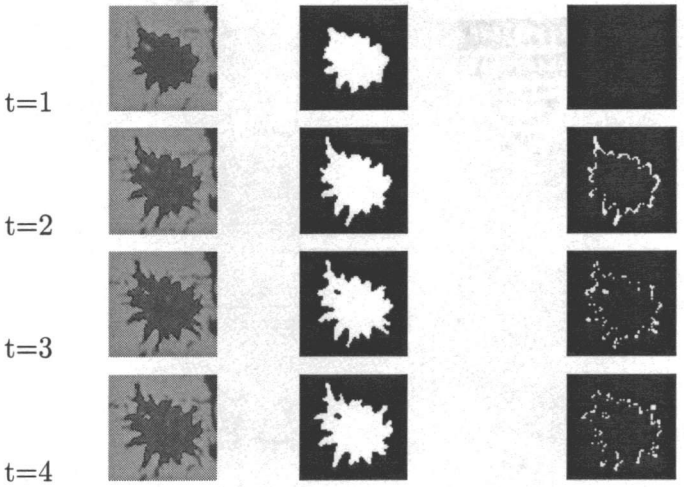

FIGURE 3.6: Dispersion of a dendritic chromatophore

3.1.2. Sequential segmentation

In this section, we specifically discuss the segmentation of image sequence depicting the changes in Chromatophore cell population. We assume that the individual cell locations can be estimated from the segmentation results of the preceding frame of the sequence. This approach does not involve object detection discussed in section 2. such detection must be performed for the first frame as part of an initialization process.

Let I_t and $I_{t+\Delta t}$ denote two consecutive RGB images from a sequence taken at the sampling rate Δt. The segmentation result of I_t is available to us as a set of regions $S_t = \{r_i^t, i = 1 \dots N\}$, r_1^t is the background region and $\{r_i^t, i = 2 \dots N\}$ are the regions of the $N-1$ cells present in the field of view at time t.

Our objective is to derive the regions $S_{t+\Delta t}$ from $I_{t+\Delta t}$ and S_t. To do so we need to generate a marker set $S'_{(t+\Delta t)} = \{r_i'^{(t+\Delta t)}, i \in \{0...N\}\}$ such that for each optimal region $r_i^{t+\Delta t}, i \in \{1...N\}$, $r_i'^{(t+\Delta t)} \subset r_i^{t+\Delta t}$. $r_0'^{(t+\Delta t)}$ will be the region of unknown class featuring the ambiguity that need to be resolved by a seeded region growing segmentation algorithm such as watershed.

We assume that the only behavior that can be expected from the chromatophores are aggregation or dispersion. From biological facts, we can obtain the maximal aggregation speed Va and the maximal dispersion speed Vd.

- If a cell r_i is undergoing a dispersion process, then r_i^t can be directly taken as a marker since $r_i^t \subset r_i^{t+\Delta t}$:
  $r_i'^{(t+\Delta t)} = r_i^t$

  In the case of the background r_1 is shrinking and we must anticipate the largest possible shrinking rate to obtain a relevant marker. To do so we must erode r_1^t using a circular structuring element S of diameter $(2 \cdot Vd \cdot \Delta t)$:
  $r_1'^{(t+\Delta t)} = r_1^t \ominus S(2 \cdot Vd \cdot \Delta t)$

- If a cell r_i is undergoing a aggregation process, we must anticipate its largest possible shrinking to obtain a relevant marker. Therefore we must erode r_i^t using a radial structuring element T (See section 3.1.1.) of length $(2 \cdot Va \cdot \Delta t)$:
  $r_i'^{(t+\Delta t)} = r_i^t \ominus T(2 \cdot Va \cdot \Delta t)$

  On the other hand the background region r_1^t can be directly used as a marker since $r_1^t \subset r_1^{t+\Delta t}$:
  $r_1'^{(t+\Delta t)} = r_1^t$

In real operating conditions, we cannot predict the cells behavior, furthermore we can be confronted with a situation where one cell type (Melanophore) is aggregating while the other (Erythrophore) is dispersing. To be able to cope with such cases, we need to combine the marker generation rules:

$$\begin{cases} r_i'^{(t+\Delta t)} = r_i^t \ominus T(2 \cdot Va \cdot \Delta t), i \in \{2...N\} \\ r_1'^{(t+\Delta t)} = r_1^t \ominus S(2 \cdot Vd \cdot \Delta t) \end{cases}$$

The global process of marker generation is illustrated in Figures 3.7 3.8 and 3.9.

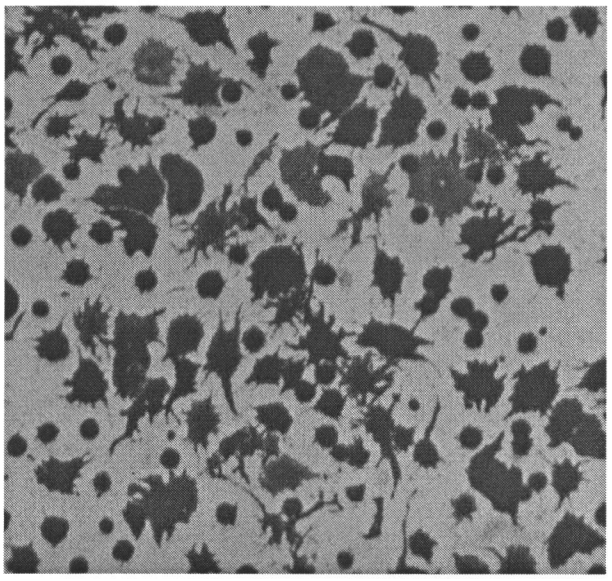

FIGURE 3.7: RGB image at frame i

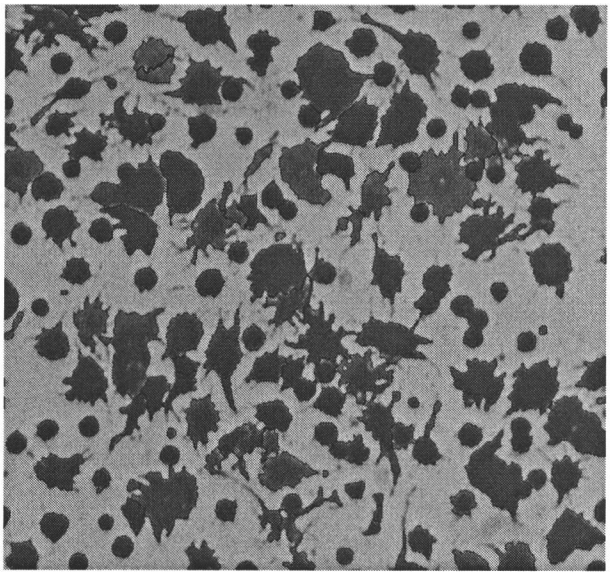

FIGURE 3.8: segmented image at frame i

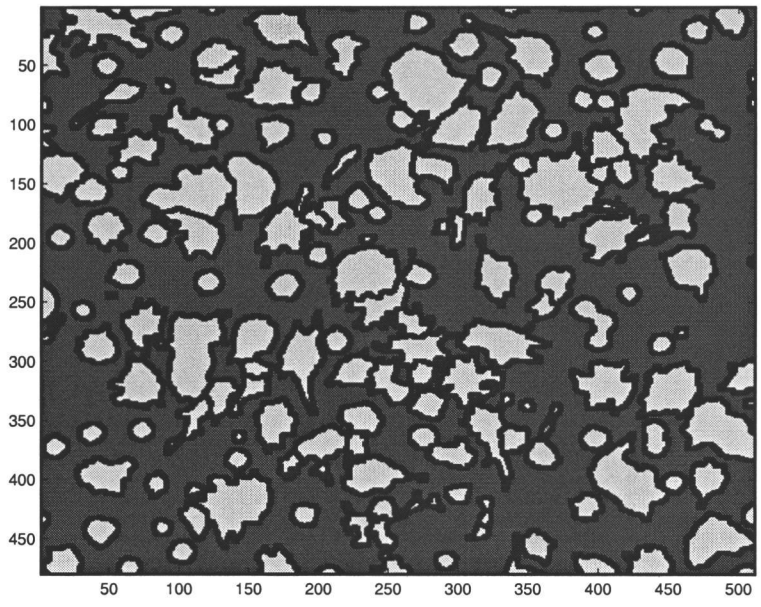

FIGURE 3.9: Marker image used for frame $i + 1$

3.2. Cell tracking strategies

Chromatophore cells under observation are maintained in a fluidic L15 environment. Theoretically, their movement is restrained by a special biological glue but it is not uncommon to see some cells breaking free and being driven by the flow of liquid during agent injection.

This phenomenon is likely to influence the marker based tracking process and impair the image segmentation. To counter these problems, we compute a cell validation Mask $CellMask$ through image binarization (Automatic thresholding) of the image under consideration I_t. This mask will be used to validate the cell marker set $S'_t = \{r'_i, i \in \{2...N\}\}$. The regions that are not validated by this mask will be flagged as background and ignored by the watershed algorithm. For the practical purposes these cells are lost.

4. CELL ANALYSIS

Region Based Image segmentation of an image sequence provides us with a mapping $(x, y, time) \rightarrow (CellId, time)$. By computing certain object features, it is possible to represent these objects in a feature space. An image sequence is therefore reduced to feature array time series.

In this part, we investigate certain features to determine which ones are most relevant to modelling and prediction.

- Geometrical analysis:

  This leads to the analysis of the shape of the cell, as defined by the binary mask computed during the segmentation process.

- Color analysis:

  The objective is to estimate the statistical model of the cell color content in a color space. Pigmentation of organelles is an important feature since it permits the differentiation between Erythrophores (red) and Melanophores (black).

- Chromatozome statistical analysis:

  In this case chromatophore cells are considered as a distribution of microscopic organelles called chromatosomes enclosed inside the cell membrane. We use the chromatosome density map (Section 2.4.1.) to analyze this distribution from a statistical point of view.

4.1. Geometrical analysis

Here, only the binary map defining the cell region is considered. Thus, this process is dedicated to computing geometrical features. At this point, we do not know exactly which features are important to correctly model cell behavior. More experiments are

needed to answer this question. Presently we compute a standard set of features (see Figure 4.1)

Let $R = \{(x_i, y_i), i = 1 \ldots N\}$ be the region composed of N pixels representing the cell to be analyzed. We compute a standard set of geometrical features:

Area	Centroid
Perimeter	Extent
Major Axis Length	Minor Axis Length
Eccentricity	Orientation
Convex Area	Euler Number
Equivalent Diameter	Solidity
ConvexHull	ConvexArea

Area which estimates the extent of the Chromatosome distribution spatial support is probably the most interesting element of this set since it provides us with an estimate of the organelle aggregation/dispersion rate.

Solidity defined as $(Area/ConvexArea)$ can be used to estimate the degree of dendricity of a cell, thus allowing us to define sub-populations of dendritic and "compact" cells.

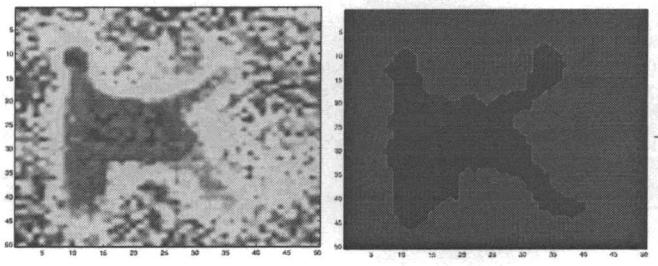

STRUCTURAL FEATURES:

Area:	611
MajorAxisLength:	36.6694
MinorAxisLength:	34.9972
Eccentricity:	0.2985
Orientation:	62.1704
ConvexArea:	1193
FilledArea:	611
EulerNumber:	1
EquivDiameter:	27.8917
Solidity:	0.5122

FIGURE 4.1: Geometrical features computation

The global set of cell regions $S = \{r_i^t, i = 2 \ldots N\}$ is defined by the labeled image resulting from the region based segmentation. If we assume a 4 or 8 pixel connectivity, we can estimate the connectivity $connect(i, j), i = 2 \ldots N, j = 2 \ldots N$ "value" between two cell regions, thus allowing us to investigate the possible interactions between cells which are in contact with each other.

4.2. Color analysis

In this case, the analysis is performed in a color space (see Figure 4.2). We assume that we are working in the RGB domain but other domains might be considered as well (e.g. HSV, Principal components).

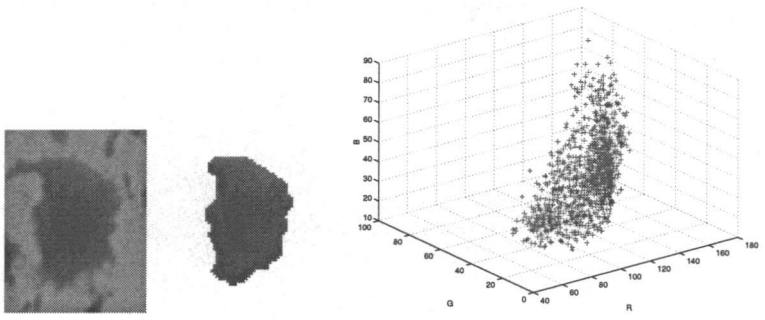

(a) (b) (c)

FIGURE 4.2: Color analysis of a cell, (a):Cell Image (b):Extracted Cell (c):Pixels of a cell in RGB space

Our final objective is to model the color distribution of each cell. To do so, two kinds of analysis are performed:

- Statistical analysis
- Fuzzy cluster analysis

4.2.1. Statistical analysis

For this analysis, we need to assume a statistical distribution of the pixels of a cell in the color space. A natural choice in our situation is to assume the distribution to be Gaussian. Therefore we aim to find the parameters of the following density function.

$$P(x) = \frac{1}{(2\pi)^{d/2}|\Sigma|^{1/2}} e^{-\frac{1}{2}(x-\mu)^T \Sigma^{-1}(x-\mu)} \tag{4.1}$$

x : RGB vector representing a pixel

μ : mean color of the cell

Σ : Correlation matrix

d : number of color bands

This gaussian density function can be easily obtained by computing the mean color μ and the Correlation matrix Σ.

The Correlation matrix is of particular interest to us because it allows to obtain the axes direction of the ellipsoids of constant density (See figure 4.3). These axes can be computed directly by performing the eigenvalue/eigenvector decomposition of Σ.

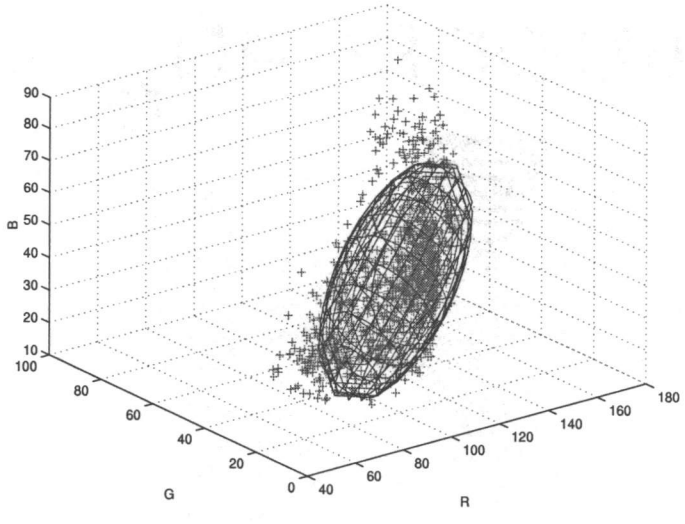

FIGURE 4.3: Ellipsoid of constant density of probability

4.2.2. Cluster analysis

The purpose of this analysis is to model color components of the cell. It can be typically divided into two regions:

- The core

  (typically darker color region)

- The periphery

  (Typically lighter color region, extend of which can vary depending on the toxic environment)

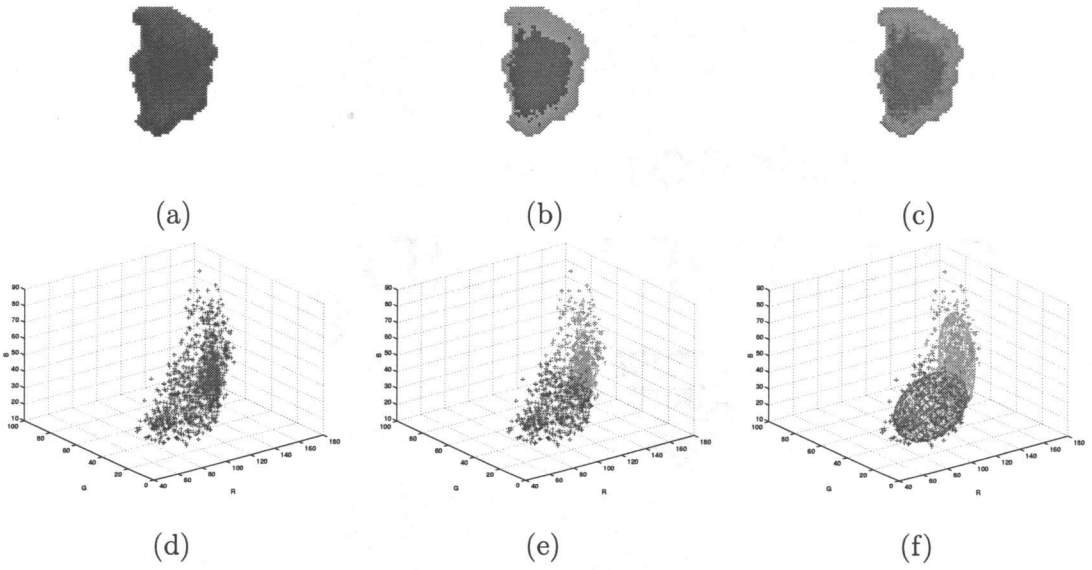

FIGURE 4.4: (a):Extracted Cell, (b):Crisp segmentation, (c):Fuzzy segmentation, (d): Pixels of a cell in RGB space, (e): Clusters display, (f): Clusters modelling

To identify these regions, the cluster analysis approach, which detects grouping within the data, is a natural choice. From large number of existing clustering techniques, we chose a variant of the fuzzy K-mean clustering to perform this operation.

In our case, the fuzzy approach is more appropriate because fuzzy cluster analysis avoids unambiguous mapping of pixel values to classes, and instead computes degrees of membership to specify to what extend data belongs to a cluster. This is of particular interest considering that the region between the core and periphery of a cell can be very shallow. Another advantage is that this method is more stable and less sensitive to local minima of the objective function used in clustering.

For the details about clustering algorithm, refer to [6]. From a practical point of view, the fuzzy C-mean algorithm computes a probabilistic cluster partition $f(p)(k)$ which can be interpreted as the probability for membership of the pixel p to a cluster k.

This partition is all we need to divide the pixels of a cell into two classes. Next these classes can be analyzed statistically (See Figure 4.4).

4.3. Chromatosome statistical analysis

In this part, we focus on the way the chromatosomes are distributed within the boundaries of the cell membrane. The organelle distribution of a cell is defined by its spatial support $R = \{(x_i, y_i), i = 1 \ldots N\}$ and its chromatosome density map d (See section 2.4.1.).

From this we can first compute the distribution weight W and center (x_m, y_w):

$$\begin{cases} W = \sum_{(x,y)\in R} d(x,y) \\ x_m = \frac{\sum_{(x,y)\in R} x \cdot d(x,y)}{\sum_{(x,y)\in R} d(x,y)} \\ y_m = \frac{\sum_{(x,y)\in R} y \cdot d(x,y)}{\sum_{(x,y)\in R} d(x,y)} \end{cases}$$

We can also compute the second moments of the distribution as a correlation matrix C:

$$C = \begin{bmatrix} \sum_{(x,y)\in R}(x-x_m)^2 d(x,y) & \sum_{(x,y)\in R}(x-x_m)(y-y_m)d(x,y) \\ \sum_{(x,y)\in R}(x-x_m)(y-y_m)d(x,y) & \sum_{(x,y)\in R}(y-y_m)^2 d(x,y) \end{bmatrix}$$

4.4. Cell monitoring

Some of the cell features that we computed can be used for static analysis purposes, i.e. to assess the nature (Melanophore, Erythrophore, dendritic, compact) of the cells when they are in their resting state.

But the key feature of the chromatophores under study is their dynamic behavior when exposed to toxic agent. This is what allows us to assess an agent toxicity and permits toxin classification and recognition. By monitoring the structure and color evolution of each individual cell, our ultimate objective is to compare these behaviors to some models so as to be able to detect and identify toxins.

To characterize the cell behavior, we will monitor the evolution of the cell features after injection of one (See Figure 4.5 and 4.6) or several agents (See Figure 4.7 and 4.8).

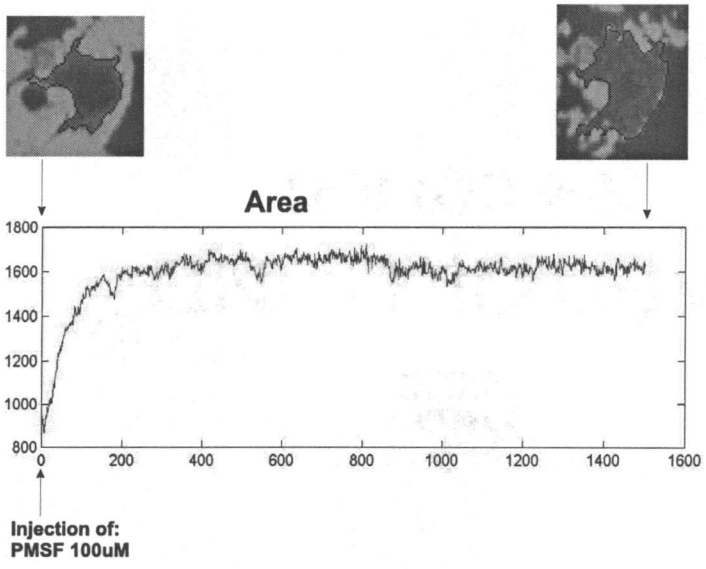

FIGURE 4.5: Monitoring of the cell area in a one-stage experiment

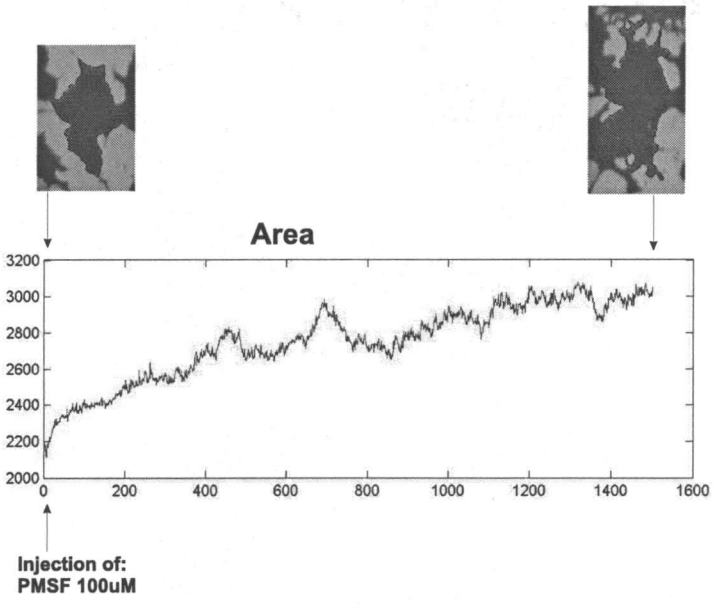

FIGURE 4.6: Monitoring of the cell area in a one-stage experiment

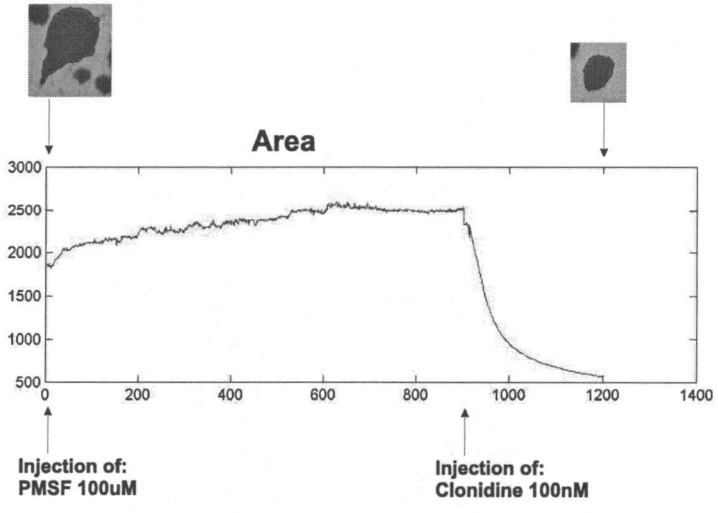

FIGURE 4.7: Monitoring of the cell area in a Two-stage experiment

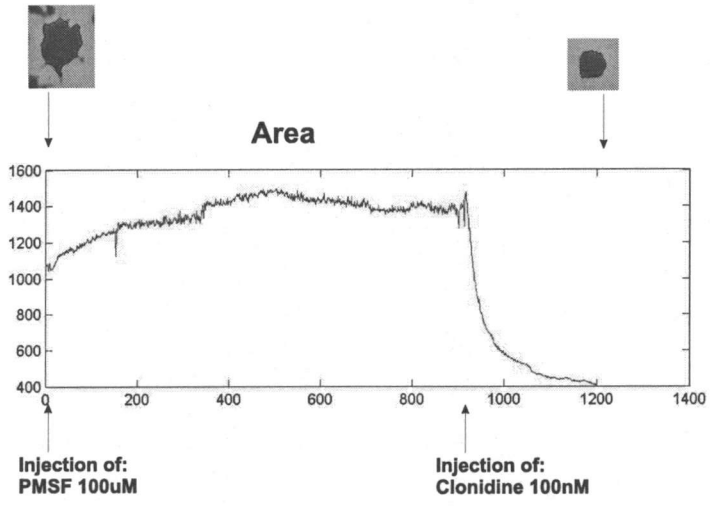

FIGURE 4.8: Monitoring of the cell area in a Two-stage experiment

5. MODELING AND CLASSIFICATION

In the previous sections, we principally discussed the concepts of tracking the changes of individual cells. To this end, an extensive number of features were computed to characterize these changes. Our major concern was segmentation reliability and stability.

In this part of the study, our intention is to extract from the previously generated raw data a set of features relevant to some specific cell behaviors. Ultimately, we want to model the feature changes.

To achieve this objective, a standardization of the cells and the experimental protocols are needed. The scope of this preliminary study is limited, since such standardization is currently under the development. Here, we only introduce the general concepts involved in cell change modeling.

5.1. Static cell classification

When exposed to some agents, chromatophore cells can react either by chromatosome aggregation or dispersion. The nature and extent of this reaction depends on the injected agent and the nature (Erythrophore, Melanophore) of the cell. For example, some experiments demonstrated that *beta amyloid*, induces aggregation on Melanophores and dispersion on Erythrophores (See Figure 5.1).

Membership to a class Erythrophore or Melanophore has to be crisp since there are no intermediate/hybrid cells containing a mix of Erythrosome and Melanozome organelles. The nature of a cell can be assessed from its associated object features, principally its color and area.

To perform this classification, we chose a simple discriminant function approach.

Lets consider $\Omega = \{\omega_1, \omega_2\}$ of 2 cell categories, and $X = [x_1, \ldots, x_n]^t$ a feature vector . The objective is to associate each class with a discriminant function $d_\lambda(x), \lambda = 1 \ldots 2$. They can be expressed in a vectorial form as:

$d_\lambda(x) = a_\lambda^t \cdot \varphi(x)$

a_λ is a parameter vector and $\varphi(x)$ is the processed features vector. Various parameterization schemes can be introduced here. We selected linear-in-parameters model so the solution takes close-form. Notice that $\varphi(x)$ can be arbitrary vectorial function of its argument. Here we chose $\varphi(x)$ as follows:

$$a_\lambda = [b_0, \ldots, b_n]^t$$
$$\varphi(x) = [1, x_1, \ldots, x_n]^t$$

Our objective is then to find the best discriminant functions $d_\lambda(x), \lambda = 1 \ldots 2$ of this family to perform the classification task.

Let us define the optimal discriminant function basis: $\{\delta_1, \ldots, \delta_2\}$ such that:

$$\begin{cases} \delta_\lambda(x) = 1 & \text{if} \quad X \in \omega_\lambda \\ \delta_\lambda(x) = 0 & \text{otherwise} \end{cases}$$

We want d_λ to be the best approximation of the ideal discriminant function δ_λ. Considering the mean squared errors

$Mse = E\{\Sigma_{\lambda=1}^2(\delta_\lambda(x) - d_\lambda(c))^2\} = E\{\Sigma_{\lambda=1}^2(\delta_\lambda(x) - a_\lambda^t \cdot \varphi(x))^2\}$

our objective is to minimize Mse.

Rewriting the expression for Mse in a matrix-based form we have

$$\begin{cases} Mse(A) = E\{(\Delta(x) - A^t\varphi(x))\} \\ \Delta(x) = [\delta_1(x), \ldots, \delta_2(x)]^t \\ A = [a_1|\ldots|a_2] \end{cases}$$

Our objective is to find the optimal parameter matrix A^* such that:

$A^* = ArgMin_A(Mse(A))$.

It can be shown that this optimal parameter matrix satisfies the following relation:

$$A^* = [E\{\varphi(x)\varphi^t(x)\}]^{-1}E\{\varphi(x)\Delta^t(x)\}$$

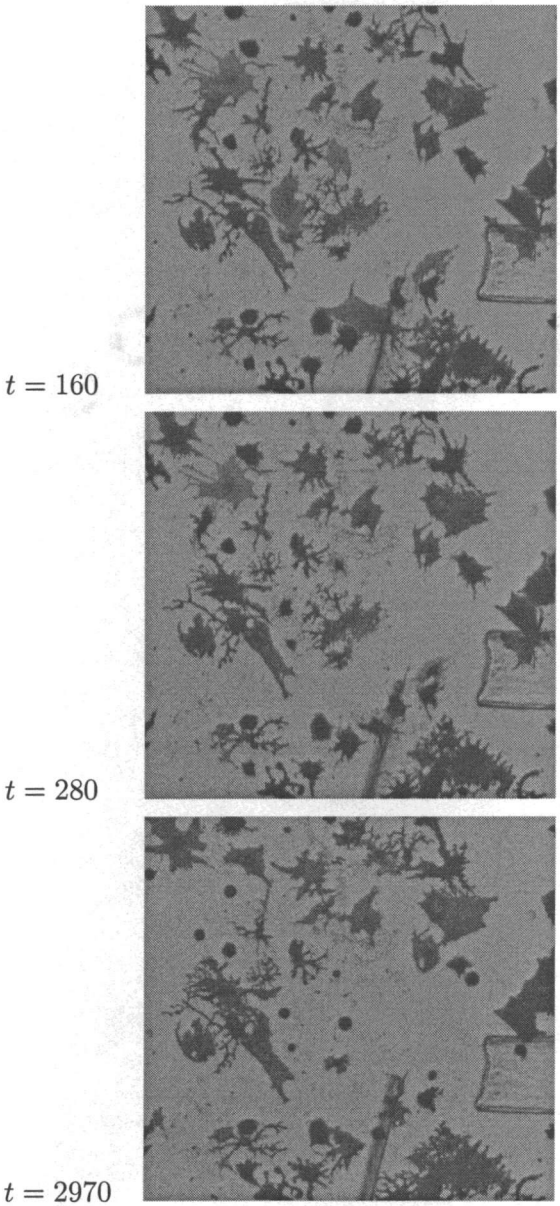

FIGURE 5.1: Cell response to beta amyloid 100 uM

The initial aggregation state of a cell can greatly influence the toxin response. An organelles aggregation agent such as Clonidine won't have any effect on a fully aggregated cell, similarly a organelle dispersion agent will not affect a fully dispersed cell.

Since cells can come in various aggregation states, our concern is more of quantification than classification. From experimental observations, we know that fully aggregated chromatophores exhibit relatively standard spatial support area (See Figure 5.2). From this fact we can obtain the typical area of fully aggregated cells $Area_{AG}$ and use it to define an estimate of the cell degree of aggregation: $\hat{Agr}$:

$\hat{Agr} = \frac{Area}{Area_{AG}}$

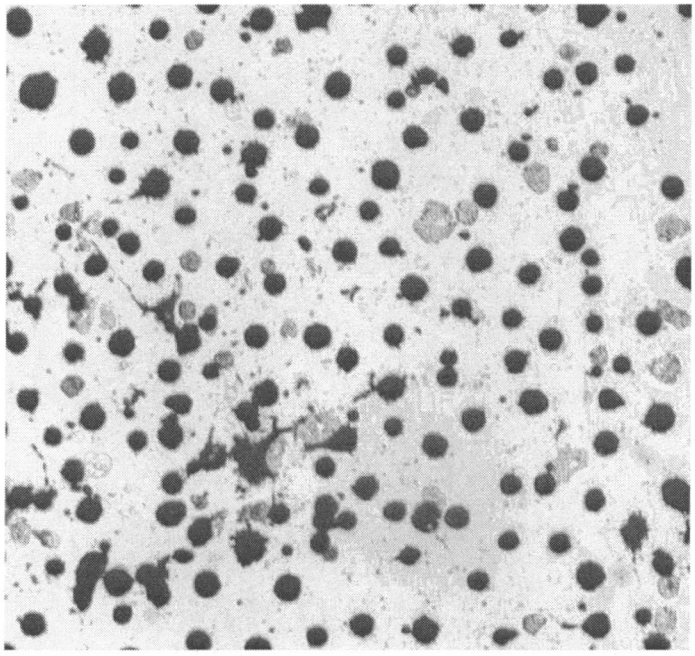

FIGURE 5.2: Population of fully aggregated cells

Finally, the initial degree of dendricity must be quantified since the membrane configuration is likely to affect the flow of chromatozomes during the aggregation or dispersion processes. As an estimate of the cell dendricity $\hat{dend}$ we used the ratio of the

area over the convex area:

$\hat{dend} = \frac{Area}{ConvexArea}$

5.2. Dynamic behavior modelling

By monitoring each cell individually, we can obtain a vectorial time series of variable length which depends on the experiment duration. Modelling such time series consists of describing them by a fixed length set of parameters called feature vector.

5.2.1. Feature preprocessing

The analysis process discussed in section 4. computes an extensive number of features to characterize each cell. This set has been developed to be as extensive as possible within the bounds of what can be computed in a relatively short time.

Any feature describing aspects of a cell is in principle relevant but our intent is to select the ones that best describe the cell internal process and to pre-process them for normalization purposes.

5.2.1.1. Feature Selection

Through the selection process discussed above, we intend to identify a subset of features relevant to the expected cell behaviors. Designing a strategy for dynamically selecting features depending on the experimental conditions is beyond the scope of this thesis. What was done in practice was to chose the features which best represent the expected cell behavior.

The currently used features include, *area*, *convexarea* and the eigenvalues $(\lambda_1, \lambda_2), \lambda_1 \geq \lambda_2$ of the correlation matrix of the cell chromatozome distribution.

5.2.1.2. Feature Extraction

Feature extraction is required for normalization purposes. As an illustration we consider some possible normalized extracted features:

- $f_1(i) = \sqrt{\frac{ConvexArea}{\pi}}$

  This feature is basically the equivalent radius er of the cell Convex Hull, it is expected to characterize the chromatosome displacement involved in the aggregation or dispersion processes. This measurement is designed to be valid on both compact and dendritic cells and is motivated by the fact that the chromatosome displacement is visible at the extremas of dendritic chromatophores.

- $f_2(i) = 2\pi[\lambda_1(i)^2 + \frac{\lambda_1(i)^2}{2e} ln(\frac{1+e}{1-e})], e = \frac{\sqrt{\lambda_1(i)^2 - \lambda_2(i)^2}}{\lambda_1(i)}$

  f_2 can be interpreted as a statistical area within the unitary variance bounds.

5.2.2. Behavior modeling

By monitoring each cell individually, we can obtain a set of time series of variable length (see figure 5.3). Modelling this series consists in describing it by a fixed length set of parameters called feature vector.

Time series modelling is the ultimate step required to perform response classification. A possible approach to this modelling is presented below.

First, note that we are not really interested in obtaining a model of the cell behavior. Modeling leads to explaining how the data is generated, which is extremely complex in this case. What we want is a **descriptor** that makes the minimal assumptions on the nature of the signal. To reach this objective, Auto-regressive (AR) processes is a possibility.

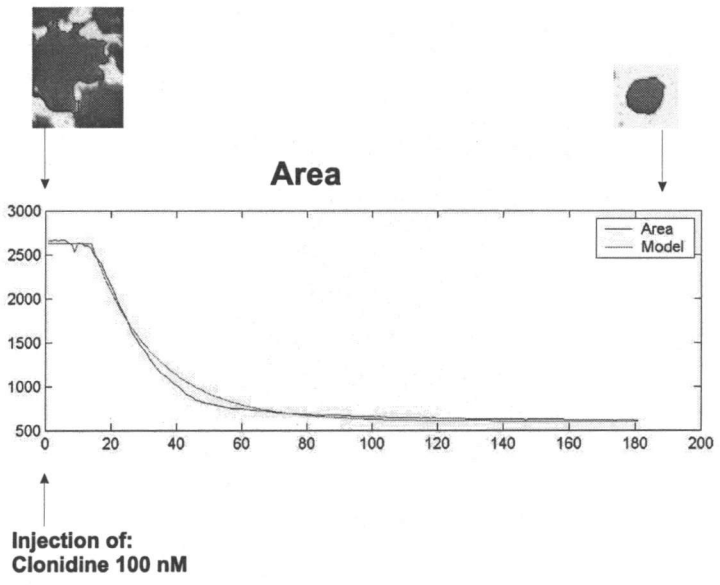

FIGURE 5.3: Evolution on a cell feature

Assuming that we have a normalized time series y featuring the response of a cell to a single agent, the evolution of y will be modelled by a order p auto-regressive process. the model y_m of y is defined as:

$$\begin{cases} y_m(t_i) = C & \text{if} \quad 0 \leq t_i \leq t_L \\ y_m(t_i) = b_0 + (\sum_{k=1}^{p} y_m(t_{i-p}) a_p) + w_i & \text{if} \quad t_L < t_i \end{cases}$$

The parameters of this model are :C, t_L,b_0, $(a_i, i = 1 \ldots p)$. They are determined in order to minimize the mean square error of the model and characterize the cell behavior. The model assumes that the cell response level remains at a constant value C for a duration t_L which determines the latency of the cell response, then actual evolution is modelled by a AR process with parameters $(a_i, i = 1 \ldots p)$ and b_0. An illustration of this modelling approach is given on Figure 5.4.

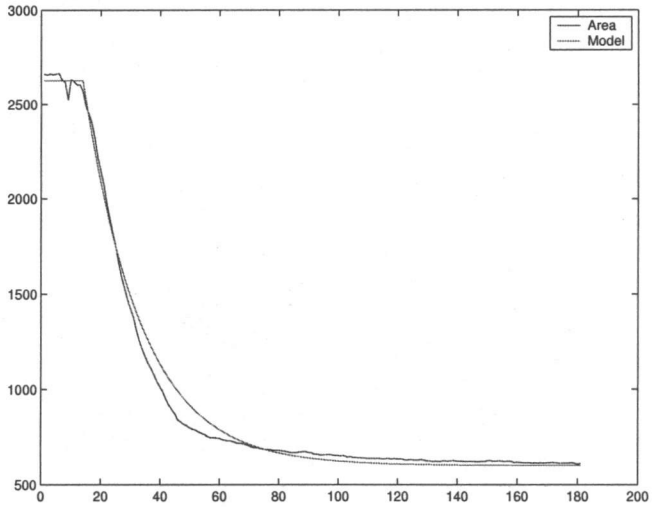

FIGURE 5.4: Original data and model of the response of a cell to a single agent

This modelling scheme applies to the situations where cells are responding to a single agent. However some experiments deal with the responses of the cells to a combination of two or more agents. In Figure 5.5, such a case is illustrated. Agent 1 is first injected and the cell response is recorded, then the operator injects Agent 2.

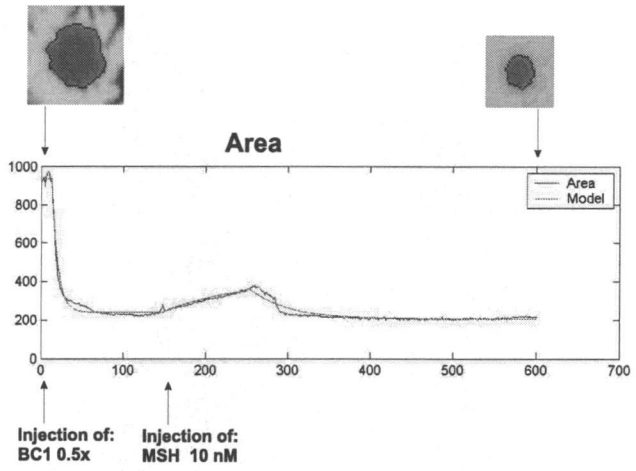

FIGURE 5.5: Evolution on a cell feature in response to two agents

The initial cell response prior to the second injection can be modeled using the single agent modelling scheme. However after the second injection, 2 different agents are present in the medium. In this situation, we decided to model this behavior using two successive AR process segments. The location of each segments is optimized in the mean square error sense (See Figure 5.6).

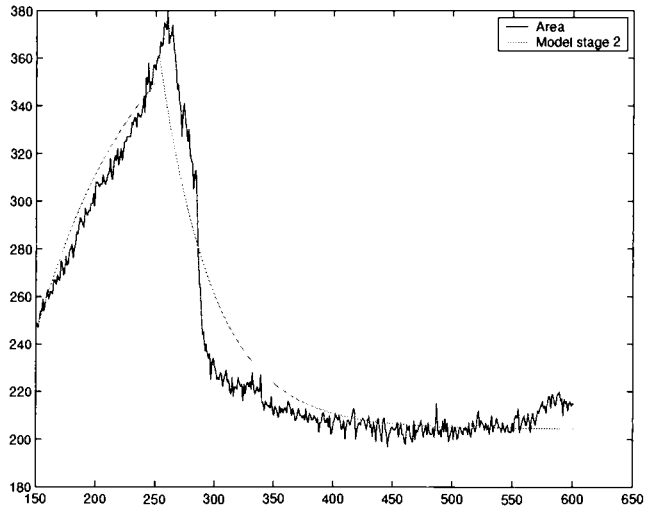

FIGURE 5.6: Original data and model of the response of a cell to two agents

Choosing the correct modelling scheme is a very important topic that will require further research.

5.3. Agent signature classification

Experimental observations suggest that the cell dynamic behavior in response to an injected agent could be used as a signature. Classification of these signatures can make toxin detection and recognition feasible.

In this last part of the thesis we describe some possible approaches to define a reliable agent signature. Early experimental results demonstrating the capability of the selected features from a classification point of view will be presented.

5.4. Agent signature

Our observations of the chromatophores suggest that the dynamic behavior of a cell subjected to a chemical or non-chemical agent can be described by four main factors.

- the evolution of the chromatosome distribution
- the agent type
- the cell family (Erythrophore ,Melanophore, dendritic, compact)
- the cell initial state

Agent type is basically the unknown variable or class C to be determined by the classification techniques. The three other factors are observation variables described by a feature vector f which is the agent signature. Our objective is to determine the agent type C based on the data f describing the observed variables. The classification performance will primarily depend on the quality of our observation and thus on the description accuracy of f.

f is a feature vector basically composed of three components:$f = [f_d, f_t, f_s]$

- f_d is a set of features describing the cell dynamic behavior when exposed to the agent C. It contains model parameters of the evolution of the various computed cell measurements.
- The f_t set describes the cell nature: Erythrophore ,Melanophore, dendritic or compact.
- The set f_s comprises various measurements assessing the initial state of a cell.

Our first approach to feature engineering was to consider that the the initial state of a cell was principally defined by its initial aggregation degree. We were assuming that cell measurement taken on the first image prior to toxin injection were a reliable estimator of the cell initial state.

However, some tests as well as visual observations demonstrated that the initial biochemical state inside the cell membrane was not entirely quantifiable through visual cell inspection. To overcome this difficulty, Prof Frank Chaplen [7] from the Bioengineering department of Oregon State University suggested that the state of a cell could be characterized by its dynamic behavior in response to a known agents called **elicitors**. [7] proposes to modify the experimental protocols by injecting the known agent some time after the injection of the toxin. Figure 5.6 illustrate such an experiment with a Bacillus Ceresus strain 1 primary agent and a MSH as the elicitor.

Model of the dynamic response to the combined effect of primary agent and elicitor constitutes a fourth feature set f_e that will improve the cell initial state description.

5.5. Simple classification test

Designing the best classification method for toxin recognition is beyond the scope of this thesis. Instead, we focus on demonstrating the capabilities of our measurements for classification purposes.

5.5.1. Training Data

Our basis for this preliminary study is a set of experiments featuring the Erythrophore response to 3 primary agents (BC1, BC5 and BC6) and one elicitor (MSH).

Definition of agent signature:

- f_d contains the first order model parameters describing the evolution of the equivalent radius er of the cell Convex Hull defined in Section 5.2.1.2.).

- Since we restricted our study to Erythrophores, f_t is limited to the level of dendriticity of the cell.
- We limited f_s to the initial cell area.
- Finally, for f_e we take the models of the evolution of er in response to the elicitor injection.

From our experimental data, we define two labelled data sets for classification purposes. The first data set called *BasicData* will contain feature vectors of the form $f = [f_d, f_t, f_s]$, leaving out the elicitor feature set. The second data set *ExtendedData* contains all the available features $f = [f_d, f_t, f_s, f_e]$. Both of these sets are normalized and tested for Bayesian classification.

5.5.2. Classification results for the basic data set

To assess the classification capabilities of the basic data set, we tested a Bayesian classifier using "leave-one-out" cross validation. We assume that classes are Gaussian distributions.

The following confusion Matrix was obtained:

	Actual	class 1	class 2	class 3
Predicted	class 1	204	36	19
	class 2	21	69	42
	class 3	22	178	160

Global classification accuracy : 57.66%

5.5.3. Classification results for the elicitor extended data set

To assess the classification capabilities of the elicitor extended data set, we tested a Bayesian classifier using leave one out cross validation. We assume that classes are Gaussian distributions.

The following confusion Matrix was obtained:

	Actual	class 1	class 2	class 3
Predicted	class 1	198	25	14
	class 2	17	122	17
	class 3	32	136	190

Global classification accuracy : 67.91%

5.6. Interpretation of the classification results

Distinguishing strains of Bacillus Ceresus using chromatophore is an extremely difficult task since they trigger similar aggregation processes. Due to the limited quantity of experimental data, we had to reduce the number of features to be classified to a minimum. Furthermore, we limited ourself to only one type of Chromatophores: the Erythrophore.

The purpose of these classification tests were not to demonstrate the absolute classification capabilities of the cells. We intended to show the classification improvement introduced by the use of elicitors, therefore demonstrating the existence of non-visible initial cell states.

6. CONCLUSION

In this thesis, our primary concern was of reliable cell detection by segmentation of color cell images. To achieve this goal, we presented a tree based approach that demonstrated good performance and stability while requiring minimal user input. These algorithms were designed to run in the real-time mode, therefore they could be coupled with existing real time video acquisition platforms.

Cell segmentation and tracking allowed us to generate time series of features. It has been conjectured that Chromatophore initial states and dynamic behaviors in response to an injected agent represent a reliable agent signature. In this thesis we presented preliminary development on signatures modelling and classification.

The results presented in this thesis are promising and demonstrate the capabilities of the biosensor approach to toxin detection and recognition. However many Chromatophores internal biochemical pathways are yet to be discovered and further research is needed on agent signature design and classification.

BIBLIOGRAPHY

1. Upinder S. Bhqllq and Ravi Iyengar, "Emergent properties of networks of biological signaling pathways," *SCIENCE*, vol. 283, pp. 381–386, January 1999.

2. D.A. Smith and R.M. Simmons, "Models of motor-assisted transport of intracellular particles," *Biophysical Journal*, vol. 80, pp. 45–68, January 2001.

3. Stan Scaroff and Lifeng Liu, "Deformable shape detection and description via model-based region grouping," *IEEE Transactions on pattern analysis and machine intelligence*, vol. 23, no. 5, pp. 475–489, May 2001.

4. Albert Oliveras Philippe Salembier and Luis Garrido, "Antiextensive connected operators for image and sequence processing," *IEEE transactions on Image processing*, vol. 7, no. 4, pp. 555–570, April 1998.

5. Xiaolin Wu, "Efficient statistical computation for optimal color quantization," 1991.

6. Frank Hopfer, Frank Klawonn, Rudolf Kruse, and Thomas Runkler, *Fuzzy cluster analysis*, John Wiley sons, 1999.

7. Personal communication with Prof Frank Chaplen from the Bioengineering department of Oregon State University, ," .

8. Pinoli JC Jourlin M, "A model for logarithmic image processing," *Journal of Microscopy*, vol. 1, pp. 21–35, 1988.

9. Luc Vincent and Pierre soille, "Watershed in digital space: An efficient elgorithm based on immersion simulations," *IEEE Transactions on pattern analysis and machine intelligence*, vol. 13, no. 6, pp. 583–598, June 1991.

10. Jos B.T.M. Roerdink and Arnold Meijster, "The watershed transform: Definitions, algorithms and parallelization strategies," *Fundamenta Informaticae*, vol. 41, pp. 187–228, 2000.

11. Phill McFadden, "Technical description of the sos cytosensor system," .

12. "The sos cytosensor system - sixth quarterly repport," .

13. Matrox Imaging, "Matrox imaging library (mil and activemil) 6.0, tutorial and help files," .

APPENDICES

A THE WATERSHED SEGMENTATION

The watershed theory as well as the algorithms used in this project are presented briefly. For more details refer to [10].

A1. Basic Concepts

The intuitive idea underlying this method comes from geography: it is that of a landscape or topographic relief which is immersed in a lake, with holes pierced in local minima. Catchments basins will fill up with water starting at these local minima, and, at points where water coming from different basins would meet, dams are built. When the water level has reached the highest peak in the landscape, the process is stopped. As a result, the landscape is partitioned into regions or basins separated by dams, called watershed lines or simply watersheds.

From the image processing point of view, this immersion can be applied to the gradient of a gray scale image, see figure A.1.

A2. Watershed segmentation algorithm

In conventional watershed algorithm, gradient image is used to segment the original image into nearly constant gray level regions. The region growing process involves adding the neighborhood pixels of regions to one of the regions. The merging criterion is the value of the gradient. Pixels are considered in the order based on gradient value. Lowest gradient pixels are processed first. If there are two neighborhood regions for a pixel then it is merged with the region with lowest distance.

In the modified watershed algorithm [9] used here, a marker image, that provides the initial seeds for regions in segmented image, is derived from the original image. The region growing process involves adding the adjacent pixels with marker. The merging

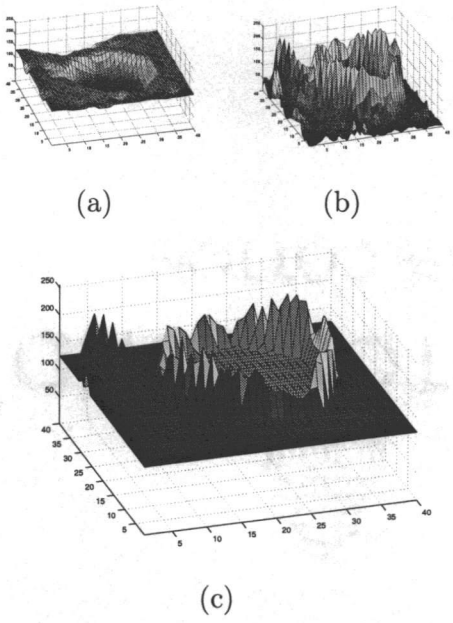

FIGURE A.1: Immersion, (a):Original Image (b):Gradient Image (c):Immersion of the gradient Image

criterion is the distance between value of pixel under consideration and the average pixel value of the region. Every time a pixel is added the average value of the pixel is updated. Pixels are processed in the order based on distance. Pixels with lower distance value are processed before pixels with higher distance.

In practice, a labelled image is used as a marker. This image (see Figure A.2) consists of zeros to mark pixels of unknown region, and positive integer to mark pixels of known region.

An interesting approach for generating the marker image is to use an approximation of the segmentation result. If such an information is available, it is relatively easy to derive the marker image by applying a binary erosion around each segment, leaving between them some uncertainty frontiers whose thickness depends on the size of the morphological operator. The task performed by the segmentation process is thus reduced to the processing of these uncertainty regions.

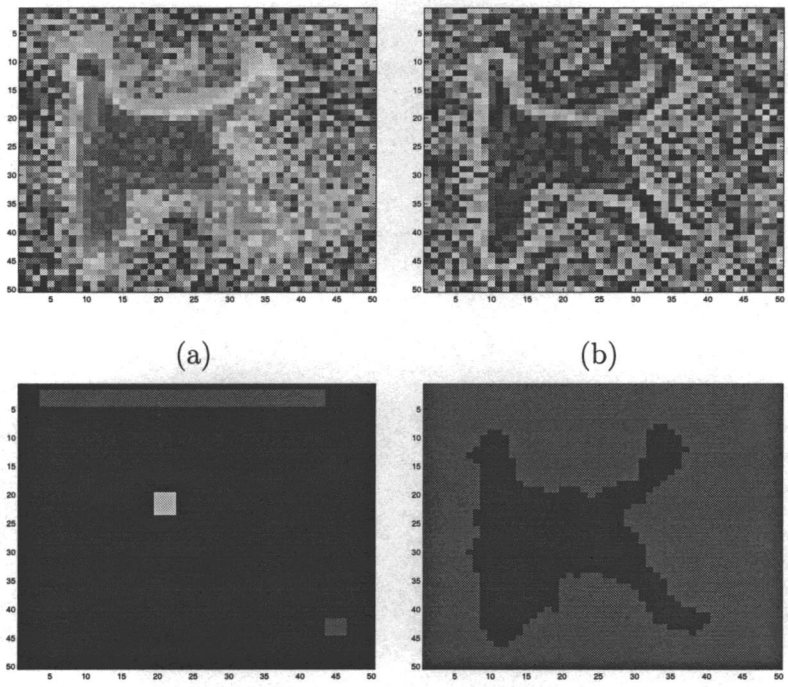

FIGURE A.2: Watershed segmentation, (a):Original Image, (b):Gradient Image, (c):Marker Image, (d):Segmentation result

This approach is very promising in our situation where we deal with sequential image data. Indeed, the approximation of the segmentation results is directly available in the form of the previously segmented frame.

In the case of the first processed frame where no prior knowledge is available, the cell detection techniques are required.

B DETECTION OF CONNECTED PIXELS IN A BINARY IMAGE

A binary image or digital grid can be seen as a special kind of graph, where the vertices are called pixels. The connectivity among the vertices are usually a 4 or 8-connectivity. Here, we assume a 4-connectivity, but its generalization to 8-connectivity is relatively straightforward.

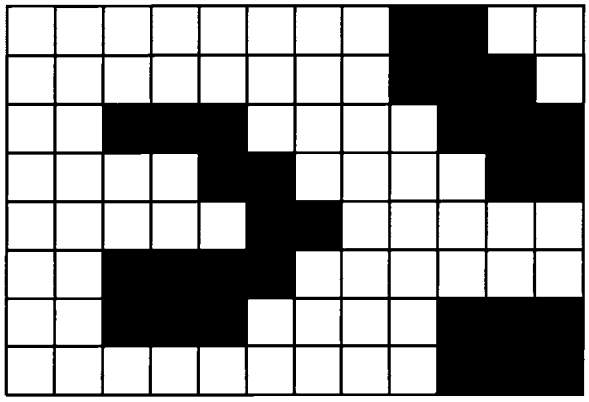

FIGURE B.1: Binary image

Our objective is to detect the connected components (marked as 1's) of the image (see figure B.1). A naive approach would be to construct a graph structure based on the image information and detect the connected components using, for example, a depth first search method. However, this would require a significant amount of memory and time.

A typical approach in such situation is to break down the problem complexity. The proposed here algorithm can be divided into several processing steps.

- **Step 1: Vertical connectivity detection**

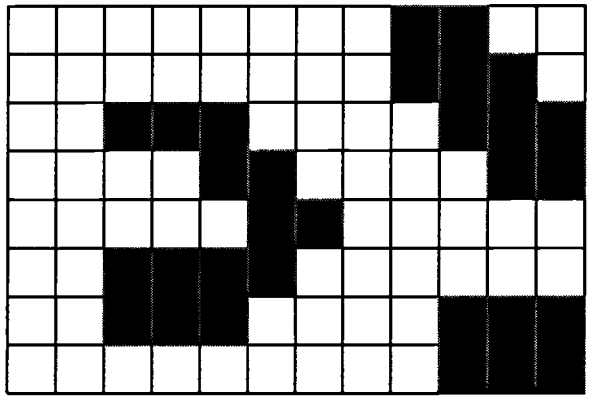

FIGURE B.2: Vertical connectivity detection

First, the image information is reduced to vertically connected components called *Runs*. Each run is defined by its column, starting line and ending line (see Figure B.2).

- **Step 2: Sub-connected components detection**

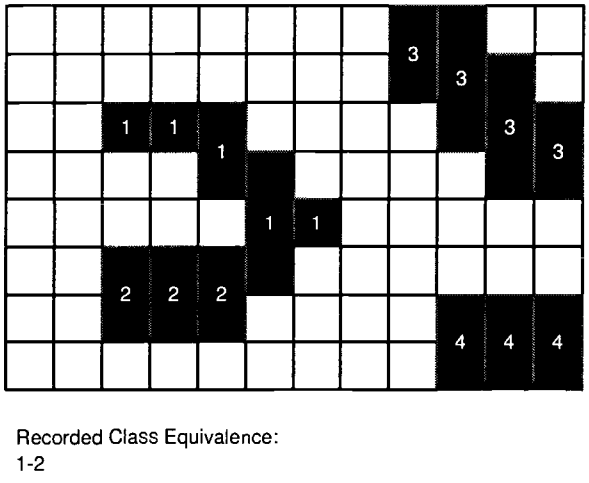

FIGURE B.3: Sub-connected components detection

At this point, runs are processed column by column(See figure B.3), the algorithm tries to associate runs of one column to the runs of the previous column. If no association is possible, then the run receives a new label. If one single association is possible, the run receive the same label as his connected counterpart from the preceeding column. Finally, if several associations are possible (conflict), the run receives the label of its first counterpart and class equivalence information is recorded.

- **Step 3: Conflict resolution**

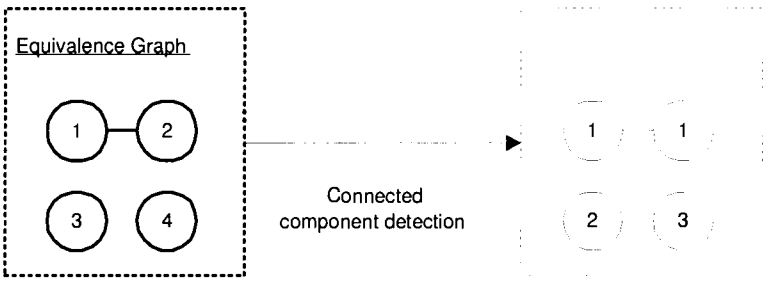

FIGURE B.4: Conflict resolution

At this point, we have sub-connected components associated with label equivalences. Based on this information, we can build a graph and perform a connected components detection using a depth first search. The sub-connected components are relabelled accordingly.

- **Step 4: Label Image reconstruction**

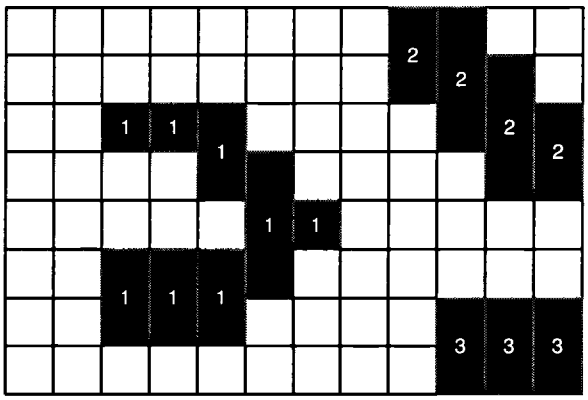

FIGURE B.5: Label Image reconstruction

The classification conflicts are now resolved, and we can next construct the labelled image.

C SINGLE CELL EVOLUTION

C1. Original

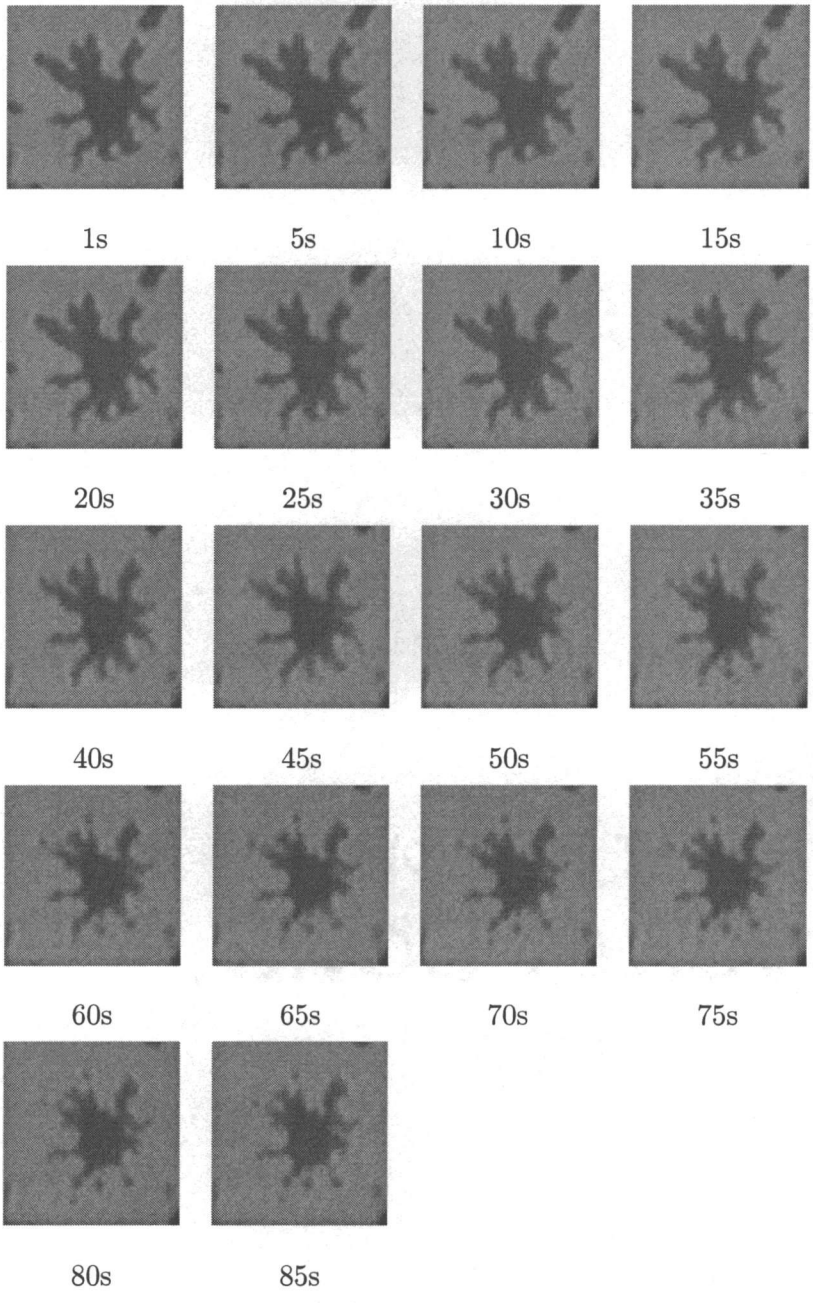

C2. Segmented

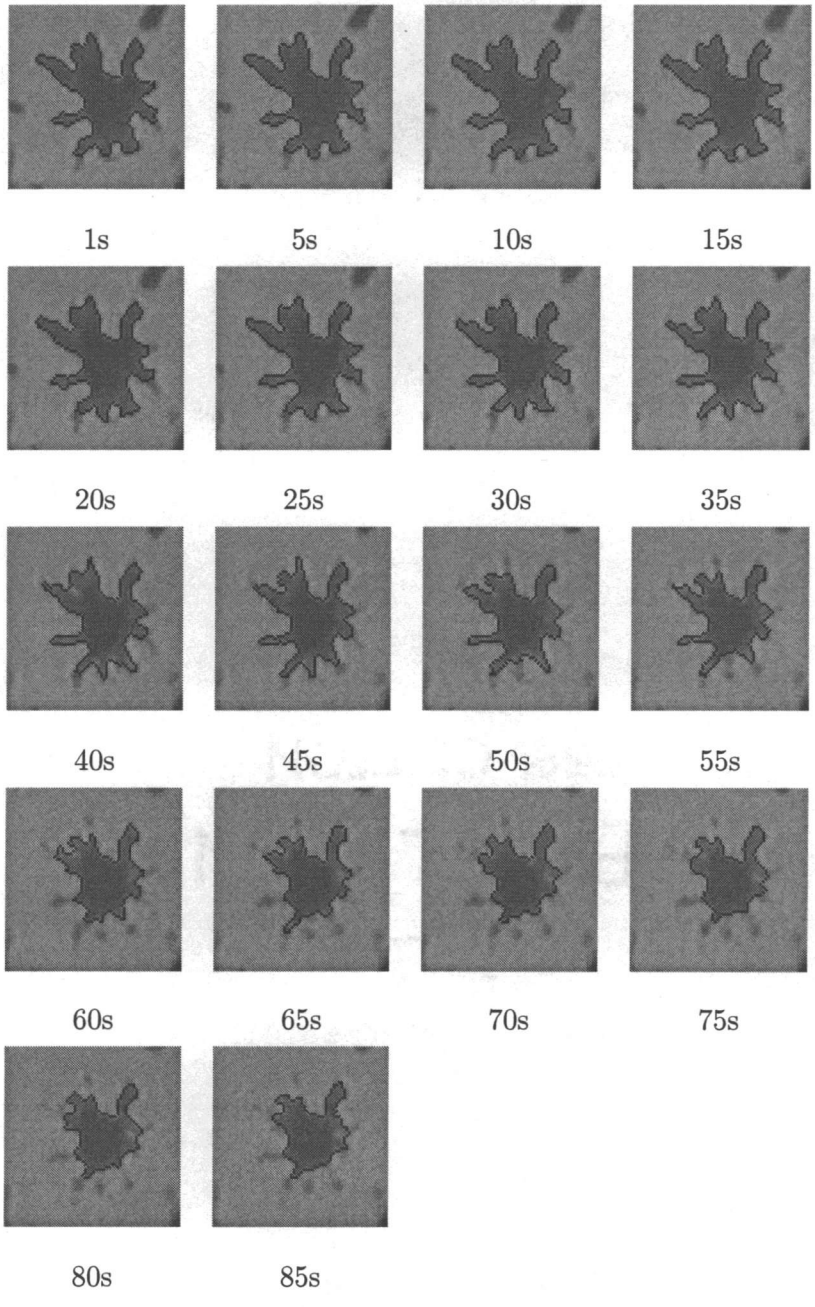

D LIP MODEL

In this part we briefly present the *Logarithmic Image Processing* (LIP) Model. For further details, refer to [8].

D1. Physical interpretation of images obtained by transmission

Basically, the LIP model applies to gray-scale images obtained by transmission across a medium. A schematic view of such an image acquisition system is presented in Figure D.1. Schematically, a light source is emitting a uniform flux of light ϕ_i which is transmitted across a medium characterized by its transmission factor $T(x)$. On the other side of the medium a non-uniform light flux $\phi_o(x)$ is emitted and captured by the camera to form the gray scale image $f(x)$.

The image f is assumed to be encoded using M gray scale levels, a common value for M is 256.

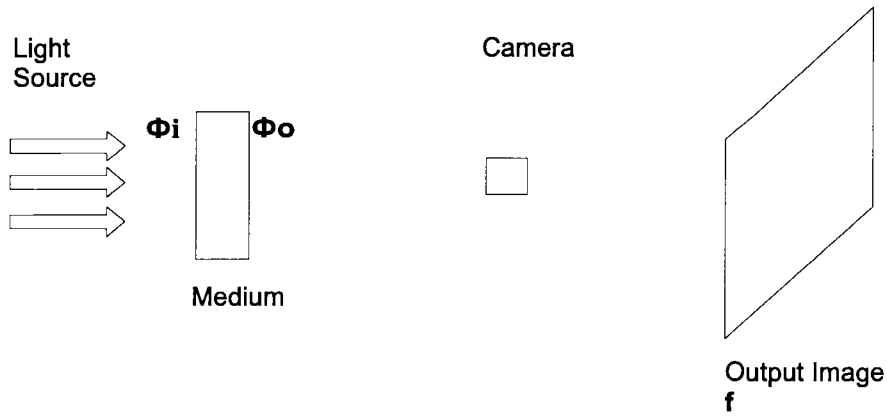

FIGURE D.1: Schematic representation of the acquisition of images obtained by transmission

We define the transmission factor of the medium as the ratio between the outgoing flux ϕ_o over the incoming flux ϕ_i:

$T(x) = \frac{\phi_o}{\phi_i}$

Let's consider the gray scale value of f at the location x:

- $f(x) = 0$ means that the medium is transparent at the location x, thus $T(x) = 1$.
- $f(x) = M$ means that no light is received at location x, therefore $T(x) = 0$

There is an inherent duality between the medium transmission factor $T(x)$ and the image $f(x)$. From a mathematical perspective, $T(x)$ can be interpreted as the probability for an incoming photon to get through the medium at location x and the duality can be mathematically defined by the formula:

$T(x) = 1 - \frac{f(x)}{M}$

D2. LIP operators

From the physical concepts discussed above, it is possible to define LIP image operators: the LIP addition $+_{LIP}$, substraction $-_{LIP}$ and multiplication $\times_{LIP}$.

D2.1. LIP addition

Assuming that a medium 1 with transmission factor T_1 produces an image f_1 and a medium 2 with transmission factor T_2 produces an image f_2, the image $(f_1 +_{LIP} f_2)$ is defined as the image that would be obtained by transmission across medium 1 and 2.

Obviously, the combined transmission across medium 1 and 2 is $(T_1 \cdot T_2)$, and using the image/transmission formula, we can mathematically define the LIP addition by:

$(f_1 +_{LIP} f_2)(x) = f_1(x) + f_2(x) - \frac{f_1(x)f_2(x)}{M}$

D2.2. LIP substraction

The transmission across medium 1 *minus* medium 2 is $\frac{T_1(x)}{T_2(x)}$, and we define the LIP substraction by:

$(f_1 -_{LIP} f_2)(x) = M(1 - \frac{1-\frac{f_1(x)}{M}}{1-\frac{f_2(x)}{M}})$

D2.3. LIP multiplication

The LIP multiplication of an image by n involves multiplying the thickness of a medium by n, the resulting transmission factor becomes $T(x)^n$ and we define the LIP multiplication by:

$(f_1 \times_{LIP} n)(x) = M - M(1 - \frac{f(x)}{M})^n$